

## RETI RANNIKU

Impact of environmental conditions  
and soil microbiome on greenhouse  
gas fluxes from soil and tree stems  
in hemiboreal drained peatland forest





## **RETI RANNIKU**

Impact of environmental conditions and  
soil microbiome on greenhouse gas fluxes  
from soil and tree stems in hemiboreal  
drained peatland forest



UNIVERSITY OF TARTU

Press

Department of Geography, Institute of Ecology and Earth Sciences, Faculty of Science and Technology, University of Tartu, Estonia

Dissertation was accepted for the commencement of the degree of *Doctor philosophiae* in geography (physical geography) at the University of Tartu on June 10, 2024 by the Scientific Council of the Institute of Ecology and Earth Sciences University of Tartu.

Supervisors: Assoc. Prof. Kaido Soosaar  
Institute of Ecology and Earth Sciences  
Department of Geography  
University of Tartu, Estonia

Prof. Ülo Mander  
Institute of Ecology and Earth Sciences  
Department of Geography  
University of Tartu, Estonia

Opponent: Prof. Vincent Gauci  
School of Geography  
Earth and Environmental Science  
University of Birmingham  
Birmingham  
United Kingdom

Commencement: Senate Hall, University Main Building, Ülikooli 18, Tartu, on August 28, 2024, at 10:15.

Publication of this dissertation is granted by the Institute of Ecology and Earth Sciences, University of Tartu.

ISSN 1406-1295 (print)  
ISBN 978-9916-27-604-4 (print)  
ISSN 2806-2302 (pdf)  
ISBN 978-9916-27-605-1 (pdf)

Copyright: Reti Ranniku, 2024

University of Tartu Press  
[www.tyk.ee](http://www.tyk.ee)

## TABLE OF CONTENTS

ORIGINAL PUBLICATIONS.....	6
ABBREVIATIONS AND ACRONYMS .....	7
ABSTRACT .....	8
INTRODUCTION.....	9
1. MATERIALS AND METHODS .....	12
1.1. Description of study site and field study design .....	12
1.1.1. Description of the study site.....	12
1.1.2. Study and experimental design .....	13
1.2. Gas sampling.....	15
1.2.1. Soil gas sampling and analysis (Article I–IV) .....	15
1.2.2. Stem gas sampling and analysis (Article I, II, III) .....	16
1.3. Flux calculations and data quality check .....	16
1.4. Environmental parameters .....	17
1.5. Soil physiochemical parameters (Articles I, III and IV) .....	17
1.6. Soil microbial community abundance (Articles III and IV) .....	17
1.7. Xylem sap flow (Article I).....	18
1.8. Dissolved gas concentrations in birch sap and soil water (Article IV) ..	18
1.9. Statistical analyses .....	18
2. RESULTS AND DISCUSSION .....	19
2.1. Soil fluxes (Article I–IV).....	19
2.1.1. Quantification and temporal dynamics of soil fluxes .....	19
2.1.2. Environmental drivers of soil fluxes.....	22
2.1.3. Effects of soil thawing on N <sub>2</sub> O fluxes.....	24
2.1.4. Soil chemistry and microbial community composition .....	25
2.2. Tree stem fluxes (Article I, II, IV).....	28
2.2.1. Quantification and temporal dynamics of stem fluxes.....	28
2.2.2. Environmental drivers of stem fluxes .....	31
2.2.3. Origin of stem fluxes .....	35
2.2.4. Relative contributions of stem and soil fluxes .....	37
3. CONCLUSIONS.....	39
REFERENCES.....	40
SUMMARY .....	49
SUMMARY IN ESTONIAN .....	52
ACKNOWLEDGEMENTS .....	55
PUBLICATIONS .....	57
CURRICULUM VITAE .....	134
ELULOOKIRJELDUS.....	136

## ORIGINAL PUBLICATIONS

This thesis is based on the following publications which are referred to in the text by Roman numerals. Published papers are reproduced in print with the permission of the publisher.

- I. **Ranniku, R.**, Mander, Ü., Escuer-Gatius, J., Schindler, T., Kupper, P., Sellin, A., Soosaar, K. (2024) Dry and wet periods determine stem and soil greenhouse gas fluxes in a northern drained peatland forest. *Science of the Total Environment*. 928, 172452.  
<https://doi.org/10.1016/j.scitotenv.2024.172452>
- II. **Ranniku, R.**, Schindler, T., Escuer-Gatius, J., Mander, Ü., Machacova, K., Soosaar, K. (2023) Tree stems are a net source of CH<sub>4</sub> and N<sub>2</sub>O in a hemi-boreal drained peatland forest during the winter period. *Environmental Research Communications*, 5, 051010.  
<https://doi.org/10.1088/2515-7620/acd7c7>
- III. Kazmi, F.A., Espenberg, M., Pärn, J., Masta, M., **Ranniku, R.**, Thayamkottu, S., Mander, Ü. (2023) Meltwater of freeze-thaw cycles drives N<sub>2</sub>O-governing microbial communities in a drained peatland forest soil. *Biology and Fertility of Soils*. <https://doi.org/10.1007/s00374-023-01790-w>
- IV. **Ranniku, R.**, Kazmi, F.A., Espenberg, M., Truupõld, J., Escuer-Gatius, J., Mander, Ü., Soosaar, K. (2024) Spring-time soil and tree stem greenhouse gas fluxes and the related soil microbiome pattern in a drained peatland forest. Submitted.

Author's contribution to the articles denotes: '\*' a minor contribution, '\*\*' a moderate contribution, '\*\*\*' a major contribution.

Categories	Author's contribution			
	I	II	III	IV
Original idea	**	**	*	**
Study design	**	**	*	***
Data processing and analysis	***	***	**	***
Interpretation of the results	***	***	**	***
Writing the manuscript	***	***	**	***

Department of Geography, Institute of Ecology and Earth Sciences, Faculty of Science and Technology, University of Tartu, Estonia.

## ABBREVIATIONS AND ACRONYMS

C	carbon
N	nitrogen
GHG	greenhouse gas
CO <sub>2</sub>	carbon dioxide
CH <sub>4</sub>	methane
N <sub>2</sub> O	nitrous oxide
<i>mcrA</i>	methyl coenzyme M reductase subunit A
<i>pmoA</i>	particulate methane monooxygenase subunit A
n-damo	nitrite-dependent anaerobic methane oxidation
<i>amoA</i>	ammonia monooxygenase subunit A
COMAMMOX	complete ammonia oxidation
<i>nirS</i>	cytochrome cd1-type nitrite reductase gene
<i>nirK</i>	copper-containing nitrite reductase gene
<i>nosZ I</i>	clade I N <sub>2</sub> O reductase gene
<i>nosZ II</i>	clade II N <sub>2</sub> O reductase gene
SWC	soil water content
WTD	water table depth
PAR	photosynthetically active radiation
NH <sub>4</sub>	ammonium
NO <sub>3</sub>	nitrate
qPCR	quantitative polymerase chain reaction
PCA	principal component analysis

## ABSTRACT

Peatlands, harbouring substantial carbon (C) and nitrogen (N) reserves, are often drained to enhance forest productivity. Drainage alters peat soil hydrology, a critical factor governing the balances of key greenhouse gases (GHGs) carbon dioxide (CO<sub>2</sub>), methane (CH<sub>4</sub>), and nitrous oxide (N<sub>2</sub>O). Lowering the water table can transform these soils from CO<sub>2</sub> sinks to sources, reduce CH<sub>4</sub> emissions, and increase N<sub>2</sub>O release. In addition to soil, tree stems play a crucial role in the GHG budgets of forestry-drained peatlands, though their dynamics are complex and understudied. Simultaneous year-long measurements of soil and tree stem GHG fluxes in northern peatland forests are rare, with previous studies primarily focusing on the growing season and neglecting seasonal variations like spring freeze-thaw cycles. Accordingly, this doctoral thesis aimed to characterise the seasonal variations and key environmental drivers of stem and soil GHG fluxes in a drained peatland forest, explore the impact of soil chemistry and microbial communities on fluxes, and provide insights into the origin of stem fluxes. Soil and stem CH<sub>4</sub>, N<sub>2</sub>O and CO<sub>2</sub> fluxes were assessed in a hemiboreal drained peatland forest, focusing on annual dynamics (Article I), wintertime fluxes (Article II), soil N<sub>2</sub>O fluxes during a freeze-thaw experiment (Article III), and springtime fluxes (Article IV). Soil GHG fluxes were determined with automated measurements using a Picarro gas analyser or manual gas sample collection and analysis with gas chromatography. Stem fluxes from downy birch (*Betula pubescens*) and Norway spruce (*Picea abies*) were quantified through manual gas sampling or measurements with portable Li-Cor gas analysers. Environmental parameters were measured simultaneously with fluxes. Soil was sampled for chemical and microbial analysis.

Soil at the study site was a net annual sink of atmospheric CH<sub>4</sub>, and a source of N<sub>2</sub>O and CO<sub>2</sub>. Soil CH<sub>4</sub> fluxes remained near-zero during the dormant season and switched to significant CH<sub>4</sub> uptake in the drier period. Soil hydrology had a long-term impact on CH<sub>4</sub> dynamics, while temperature played a more short-term role. Temporal soil N<sub>2</sub>O flux dynamics were driven by hot moments of emissions, induced by rapid changes in soil water content, such as freeze-thaw events. Soil thawing increased N<sub>2</sub>O emissions, primarily due to incomplete denitrification under prolonged anaerobic conditions. Tree stems were primarily emitters of all gases, with birch stems playing a more significant role than spruce stems. Stem CH<sub>4</sub> and N<sub>2</sub>O fluxes exhibited isolated emission peaks, driven by prolonged wetter periods for CH<sub>4</sub> and rapid hydrological changes for N<sub>2</sub>O. Both soil and stem CO<sub>2</sub> release followed a seasonal pattern, with fluxes highly dependent on temperature and linked to plant phenological and physiological activity. Stem-emitted GHGs likely had a predominantly belowground origin. Stem CH<sub>4</sub> emissions offset nearly a third of the soil sink annually, rising to almost half during wetter periods, highlighting the strong impact of soil hydrological conditions on CH<sub>4</sub> dynamics. Stem N<sub>2</sub>O fluxes responded to short-term hydrological changes, and their contribution to total N<sub>2</sub>O emissions remained low. CO<sub>2</sub> efflux from the stems accounted for most of the annual combined soil and stem flux. These findings underscore that neglecting stem fluxes can lead to inaccurate estimations of forest GHG budgets.

## INTRODUCTION

Peatlands, characterised by predominantly waterlogged conditions, cover approximately 3% of the Earth's land surface (Xu et al., 2018). These wetland ecosystems harbour substantial reserves of carbon (C) and nitrogen (N) in their soils, storing about one-third of global soil C and 12–21% of global soil organic N (Frolking et al., 2011; Limpens et al., 2006). The stability of these C and N pools is critical, as their destabilisation could significantly impact local biogeochemical cycles and global climate. Peatlands play a pivotal role in regulating key greenhouse gases (GHGs) such as carbon dioxide (CO<sub>2</sub>), methane (CH<sub>4</sub>), and nitrous oxide (N<sub>2</sub>O). Intact peatland soils typically exhibit atmospheric CO<sub>2</sub> uptake, moderate CH<sub>4</sub> release, and low N<sub>2</sub>O emissions (Frolking et al., 2011; Hugelius et al., 2020).

However, drainage aimed at enhancing forest productivity is a common practice in peatlands in the northern hemisphere, resulting in the establishment of drained peatland forests. Drainage alters soil hydrology, a critical factor governing GHG balances in peatlands (Korkiakoski et al., 2019; Lohila et al., 2011; Pihlatie et al., 2010). The transition from anaerobic to aerobic soil conditions following groundwater table lowering can transform peatland soils from a CO<sub>2</sub> sink to a source, decrease CH<sub>4</sub> emissions, and increase N<sub>2</sub>O release (Korkiakoski et al., 2019; Lohila et al., 2011; Pihlatie et al., 2010). The continuous drying of peatlands is likely to have a net global warming effect due to increased CO<sub>2</sub> and N<sub>2</sub>O emissions surpassing the impact of reduced CH<sub>4</sub> emissions (Huang et al., 2021).

In addition to soil fluxes, tree stems play a crucial role in the GHG budgets of forested ecosystems, such as forestry-drained peatlands, exchanging CO<sub>2</sub>, CH<sub>4</sub>, and N<sub>2</sub>O with the atmosphere (Barba et al., 2019; Machacova et al., 2016; Wang et al., 2019). Despite their importance, stem flux dynamics remain challenging due to spatio-temporal variability and upscaling difficulties. Consequently, most GHG models and assessments have overlooked stem contributions.

Long-term measurements of stem fluxes displaying annual dynamics are scarce (Jeffrey et al., 2023b; Machacova et al., 2019; Mander et al., 2022). Previous research has primarily focused on short measurement periods during the growing season (Barba et al., 2021; Gauci et al., 2010; Wen et al., 2017). However, recent findings showing detectable stem CH<sub>4</sub> emissions (Pangala et al., 2015) and significant N<sub>2</sub>O fluxes (Machacova et al., 2019) during winter, as well as the substantial contribution of autumn and spring fluxes to cumulative annual N<sub>2</sub>O emissions (Mander et al., 2021) underscore the importance of investigating the seasonal variability of stem fluxes and their environmental drivers. Furthermore, spring freeze-thaw cycles have been shown to be crucial in regulating temporal GHG dynamics in forested wetland and peatland ecosystems. Fluctuations in the water table associated with freeze-thaw cycles can trigger hot moments of N<sub>2</sub>O emissions from both soil and tree stems (Barrat et al., 2021; Mander et al., 2021). With climate change likely increasing the frequency of freeze-thaw events in northern latitudes (Henry, 2008), it is crucial to study springtime soil and stem GHG dynamics to better understand their underlying processes during this critical period.

Various biophysical mechanisms govern soil and stem GHG production and consumption. The net soil CH<sub>4</sub> flux is the combined result of methanogenesis and methanotrophy co-occurring in the soil, depending on the hydrological conditions (Ni & Groffman, 2018). CH<sub>4</sub> is produced in the soil microbially under anaerobic conditions by methanogenic archaea possessing the *mcrA* gene. Concurrently, CH<sub>4</sub> is consumed under aerobic conditions by methanotrophs holding the *pmoA* gene, as well as by ammonium-oxidising bacteria (Hanson & Hanson, 1996; Veldkamp et al., 2013). In addition, nitrite-dependent anaerobic methane oxidation (n-damo) has been shown to convert CH<sub>4</sub> to CO<sub>2</sub> in wetlands in the presence of excess nitrate (Hu et al., 2014).

N<sub>2</sub>O is produced in the soil through microbial nitrification and denitrification pathways (Butterbach-Bahl et al., 2013). Nitrification occurs aerobically, where specific nitrifier microbes carrying the *amoA* gene oxidise ammonia to nitrite and then nitrate, with N<sub>2</sub>O as a byproduct. On the other hand, denitrification takes place under anaerobic conditions, where, first, denitrifying microbes possessing the *nirS* and *nirK* genes reduce nitrates to N gases, including N<sub>2</sub>O. The second and final step of denitrification involves denitrifiers carrying the *nosZ I* and *nosZ II* genes, two divergent clades of N<sub>2</sub>O reducers, which convert N<sub>2</sub>O to N<sub>2</sub> gas (Kuypers et al., 2018). Hence, the net N<sub>2</sub>O flux from the soil is determined by the balance of these production and consumption processes (Braker & Conrad, 2011).

Autotrophic and heterotrophic respiration processes are responsible for the release of CO<sub>2</sub> from the soil. Autotrophic respiration from plant roots releases CO<sub>2</sub> into the soil, accumulating in soil pores or dissolving in soil water before diffusing into the atmosphere (Jiang et al., 2020; Schindlbacher et al., 2009). Autotrophic respiration also encompasses the metabolism of aboveground plants, such as trees. Heterotrophic respiration, on the other hand, involves the decomposition of soil organic matter by microorganisms such as bacteria, fungi, and archaea, which oxidise C stored in organic matter and release CO<sub>2</sub> as a byproduct (Minkinen et al., 2007; Schindlbacher et al., 2009).

The exchange of GHGs in the soil-tree-atmosphere continuum is regulated by a combination of different environmental factors. Soil GHG balance is governed by soil temperature, soil water content (SWC), water table depth (WTD), and nutrient availability (Mander et al., 2022; Mander et al., 2021; Schindler et al., 2020). The GHGs produced in the soil can then be dissolved in soil water and absorbed by plant roots, depending on root system density and depth (Bachofen et al., 2024; Puhe, 2003). Further gas transport within tree stems is governed by xylem sap flow, which facilitates the movement of gases upward via the xylem due to pressure differences.

Previous studies have shown evidence for both soil origin of stem fluxes and stem-produced fluxes (Barba et al., 2024). Soil-derived fluxes of CH<sub>4</sub>, N<sub>2</sub>O and CO<sub>2</sub> occur as water absorbed by tree roots from the soil ascends through the xylem, driven by a negative pressure induced by transpiration from the leaves. Consequently, gases dissolved in the soil water move up the stem and can diffuse into the atmosphere through the bark (Jeffrey et al., 2023b; Pangala et al., 2015; Sjögersten et al., 2020). However, microbial CH<sub>4</sub> production and consumption can

occur within terrestrial plants, including tree stems (Gauci et al., 2010; Keppler et al., 2006; Wang et al., 2016). The presence of both methanogenic and methanotrophic microbial communities has been detected in tree tissues (Putkinen et al., 2021; Yip et al., 2019), and CH<sub>4</sub> and N<sub>2</sub>O production (Lenhart et al., 2015) and N<sub>2</sub>O consumption (Machacova et al., 2017) has been demonstrated from cryptogamic covers on stem bark. Additionally, stem CO<sub>2</sub> efflux is influenced by the respiration of tree stems (Gansert & Burgdorf, 2005; Salomón et al., 2021). The dominant source of net stem flux varies depending on environmental and hydrological factors specific to each ecosystem. In wetlands, stems have been shown to act as conduits of soil-produced CH<sub>4</sub> (Covey & Megonigal, 2019; Pangala et al., 2013; Sjögersten et al., 2020), while in upland forests with drier soils, stem production could be a more dominant pathway (Pitz & Megonigal, 2017; Yip et al., 2019). However, further research is still needed to comprehensively understand the interplay between these sources of stem fluxes across different ecosystems and under varying environmental conditions.

The aims of the doctoral thesis are to:

1. Quantify and characterise the temporal dynamics of tree stem and soil CH<sub>4</sub>, N<sub>2</sub>O and CO<sub>2</sub> fluxes in a drained peatland forest (Articles I, II and IV);
2. Determine the key environmental factors governing the GHG flux dynamics from soil and stems during different seasons (Articles I–IV);
3. Understand the underlying soil chemistry and microbial communities at the study site and their potential impact on GHG fluxes (Articles I, III and IV);
4. Study the origin of stem fluxes in a drained peatland forest (Articles I, II and III).

Accordingly, the following hypotheses were proposed:

- I. There are higher CH<sub>4</sub> and N<sub>2</sub>O emissions from soil and tree stems during winter and spring;
- II. Soil hydrological parameters are the primary drivers of soil and stem fluxes;
- III. Denitrifiers drive soil N<sub>2</sub>O emissions during the freeze-thaw period;
- IV. Stem fluxes decrease with increasing stem height, indicating soil origin of stem fluxes.

# 1. MATERIALS AND METHODS

## 1.1. Description of study site and field study design

### 1.1.1. Description of the study site

The study was conducted in eastern Estonia at a drained peatland forest site (58°17'N, 27°17'E; 38 m.a.s.l.; 1.72 ha) located in the Järvelja forest district (Figure 1). The site belongs to the warm summer humid continental climate zone according to the Köppen classification (Köppen, 1936) and the hemiboreal vegetation zone, serving as a transitional region between temperate and boreal climates (Ahti et al., 1968). The region experiences an average annual precipitation of 650 mm, with temperatures averaging 17 °C in July and -6.7 °C in January and a growing season lasting 175–180 days (Kupper et al., 2011).

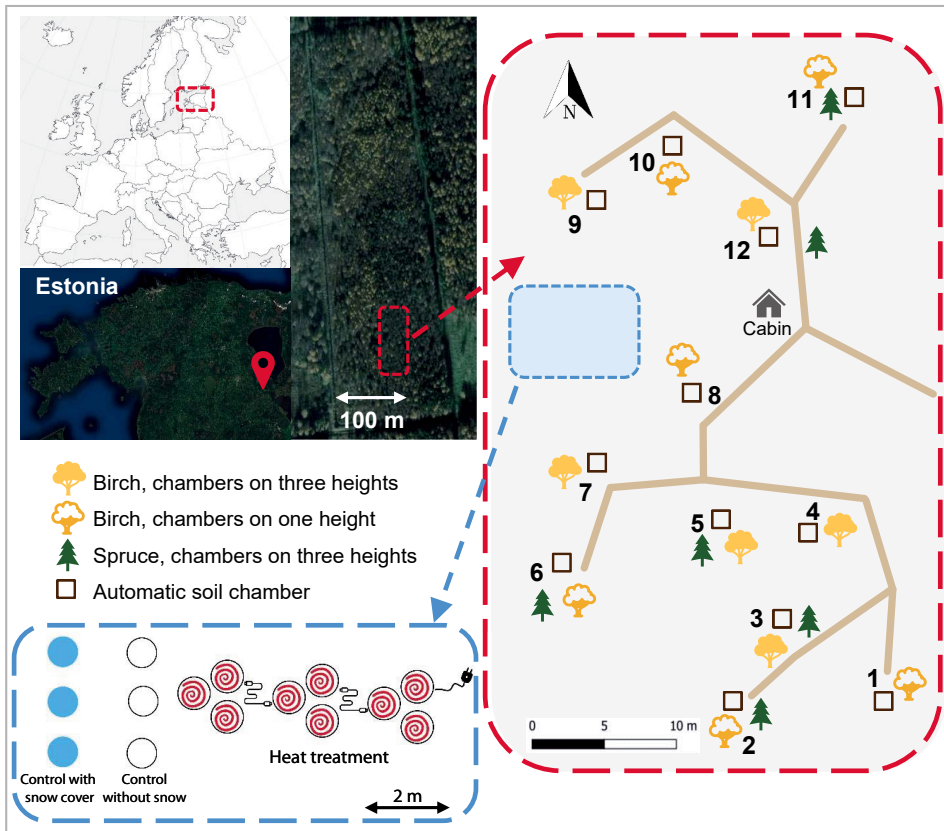


Figure 1. Location of the study area and schematic view of the study site, including numbered monitoring points with soil chambers, birch, and spruce trees. The blue rectangle represents the location and experimental scheme of the freeze-thaw experiment (Article III), showing sampling spots with different treatment conditions.

Originally a nutrient-rich fen, the site was drained in the late 1960s and early 1970s through an open-ditch network drainage system (Uri et al., 2017). The well-decomposed peat soil at the study site is classified as Drainic Eutric Histosol (IUSS Working Group WRB, 2015), with a peat layer depth of 100 cm, featuring low dry bulk density, and high N and organic C content (Uri et al., 2017). Currently, the *Oxalis*-type (Löhmus, 1984) drained peatland forest is covered mainly by a 37-year-old downy birch (*Betula pubescens* Ehrh.) stand, followed by Norway spruce (*Picea abies* (L.) H. Karst.) trees. The forest has been unmanaged since drainage (Uri et al., 2017). Forest understory vegetation is dominated by *phragmites australis* (Cav.) Trin. ex Steud., *oxalis acetosella* L., *filipendula ulmaria* (L.) Maxim., followed by *matteuccia struthiopteris* (L.) Tod., *urtica dioica* L., *rubus idaeus* L., *stellaria nemorum* L., *geum urbanum* L. and *glechoma hederacea* L.

### 1.1.2. Study and experimental design

Sampling for Articles I (study period October 2020 – December 2021), II (October 2020–May 2021) and IV (April–May 2023) was performed from twelve monitoring points located in a 50 × 70 m study plot within the total study area, detailed in Figure 1. All monitoring points consisted of an automatic dynamic soil chamber and a birch tree with installed stem chambers (Figure 2A). Six points additionally contained a spruce tree with chambers. Stem chambers were installed at heights of 0.1, 0.8 and 1.7 m above the ground to capture the vertical stem flux profile, except for six birch trees with chambers only at the lowest height.

A soil freeze-thaw experiment was conducted for Article III in March 2022. 15 soil collars with a 0.5 m diameter were installed – 12 in the soil and three on the snow (Figure 1). Nine collars had heating cables on the ground surface to induce thawing of the frozen topsoil layer (Figure 2D). The remaining six collars served as controls – three without snow and three covered with snow (Figure 2C). The freezing and thawing cycles were induced on three days, during which GHG sampling was performed. Heating was turned off overnight to ensure topsoil freezing.

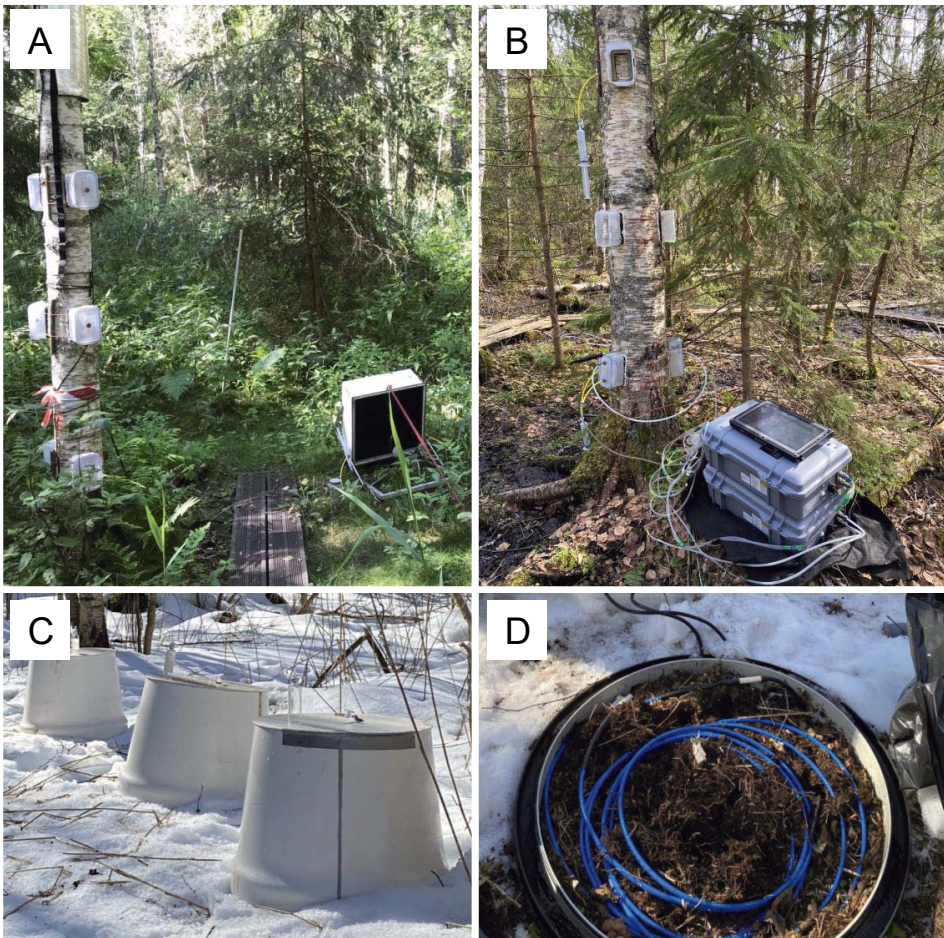


Figure 2. Photos illustrating the drained peatland forest study site. Measurement set-up of (A) automated dynamic soil chamber systems and static stem chambers on three heights used in Articles I, II and IV, (B) stem chamber systems connected to Li-Cor gas analysers and birch sap collection in Article IV, (C) soil chambers for manual soil gas sampling on snow cover used in Article III, and (D) soil collars equipped with heating cables used in Article III. Photo credit: Reti Ranniku

## 1.2. Gas sampling

### 1.2.1. Soil gas sampling and analysis (Article I–IV)

Automated soil gas measurements were performed simultaneously with stem gas sampling for Article I, II and IV. Each monitoring point was equipped with an automated dynamic opaque soil chamber made of polymethyl methacrylate, adjacent to the studied trees (Figure 2A). Chambers were connected to a multiplexer located in a cabin on-site, facilitating automated continuous gas measurements, whereby the chambers closed sequentially for nine minutes each, followed by a one-minute flushing period with ambient air. Air from the closed chamber was sampled and analysed with a gas analyser using cavity ring-down spectroscopy technology to continuously analyse CO<sub>2</sub>, CH<sub>4</sub> and N<sub>2</sub>O concentrations. The specific characteristics of each chamber system and measurement methodology are presented in Table 1.

Table 1. Soil and stem gas sampling method, chamber dimensions, gas analysis equipment

		Article I–II	Article III	Article IV
Sampling	Soil	Automatic	Manual	Automatic
	Stem	Manual	–	Manual
Chamber area m <sup>2</sup>	Soil	0.16	0.196	0.16
	Stem	0.0108	–	0.0108
Chamber volume m <sup>3</sup>	Soil	0.032	0.065	0.032
	Stem	0.00119	–	0.00119
Analysis and manufacturer	Soil	Gas analyser, G2508, Picarro Inc., Santa Clara, California, USA	Gas chromatography, GC-2014, Shimadzu, Kyoto, Japan	Gas analyser, G2508, Picarro Inc., Santa Clara, California, USA
	Stem	Gas chromatography, GC-2014, Shimadzu, Kyoto, Japan	–	Gas analyser, LI-7810 (CO <sub>2</sub> and CH <sub>4</sub> ), LI-7820 (N <sub>2</sub> O), Li-Cor Biosciences, Lincoln, NE, USA

Manual gas sampling from static soil chambers was utilised for the freeze-thaw experiment (Article III). Gas samples were collected from static polyvinyl chloride chambers placed on pre-installed collars (Figure 2C; 2D). Sampling sessions were performed from the heating plots at three timepoints: before heating (S1), after two hours of heating (S2), and after four hours of heating (S3). Control plots were sampled once per day. During each sampling session, four gas samples were drawn from the chambers with a syringe during one hour at 20-minute intervals and injected into 50 ml pre-evacuated glass bottles.

### 1.2.2. Stem gas sampling and analysis (Article I, II, III)

Manual gas sampling for stem flux quantification was conducted for Articles I and II. Gas sample collection was performed weekly from static chamber systems installed on tree stems (Figure 2A). Each chamber system comprised two chambers per height profile, positioned randomly across 180°. Stem chambers, made of transparent rectangular plastic containers (Lock & Lock, Seoul, South Korea), were affixed to the stem surface. Sampling involved closing each chamber with a removable airtight lid, using a syringe to collect a mixed 25 ml gas sample from each chamber system via septum, and injecting the sample into a pre-evacuated 20 ml glass vial. Sampling was performed from each chamber system during three hours at 60-minute intervals.

The stem gas sampling in Article IV was performed from the same stem chamber systems as used for manual sample collection. Stem chambers were closed with lids during the five-minute measurement time. Gas concentrations in the chambers were detected using portable trace gas analysers (Table 1; Figure 2B), connected to the chamber system with nylon tubing, circulating the air in a closed loop between the chamber and the analyser.

Manually collected soil and stem gas samples were analysed in the laboratory using gas chromatography, equipped with a flame ionisation detector for CH<sub>4</sub> and an electron capture detector for CO<sub>2</sub> and N<sub>2</sub>O concentrations.

### 1.3. Flux calculations and data quality check

Soil and stem CO<sub>2</sub>, CH<sub>4</sub> and N<sub>2</sub>O fluxes were calculated according to the ideal gas law and the linear regression of the gas concentration change in the chamber over time using the following equation:

$$F = \frac{M \times P \times V \times \sigma v}{R \times T \times t \times A \times f^1}$$

where F = gas flux rate, M = molecular mass of the gas (M<sub>CO<sub>2</sub></sub> = 44 g mol<sup>-1</sup>, M<sub>CH<sub>4</sub></sub> = 16 g mol<sup>-1</sup>, M<sub>N<sub>2</sub>O</sub> = 44 g mol<sup>-1</sup>), P = air pressure (101 300 Pa), V = chamber volume (m<sup>3</sup>), σv = linear regression slope of gas concentration change (ppm(v)), R = ideal gas constant (8.314 m<sup>3</sup> Pa K<sup>-1</sup> mol<sup>-1</sup>), T = temperature in the laboratory (°K), t = measurement time (h), A = soil or stem surface area covered by the chamber (m<sup>2</sup>), f<sup>1</sup> = ratio of an element in the compound.

The quality of the measurements sessions was validated using the adjusted R<sup>2</sup> value of the linear regression for the CO<sub>2</sub> measurements, which certifies chamber closure quality. Flux values were accepted if the R<sup>2</sup> value exceeded 0.9. To assess the relative contributions of soil and stem fluxes (Articles I and II), stem fluxes averaged across three heights were upscaled to a hectare of ground area, calculated based on tree stand characteristics, assuming a cylindrical shape of the tree, considering only stem fluxes that temporally coincided with soil flux measurements (4 December 2020–19 August 2021).

## 1.4. Environmental parameters

Soil and air temperature, SWC and WTD were continuously measured at half-hour intervals during the study periods in Articles I, II and IV. Soil temperature (107, Campbell Scientific, Inc, Logan, UT, USA) and soil moisture sensors (ML3 ThetaProbe, Delta-T Devices, Cambridge, United Kingdom) were placed at 0.1 m soil depth next to the soil chambers. WTD was observed in groundwater wells using automatic water level data loggers (Hobo U20L-04, Onset Computer Corporation, Bourne, Massachusetts, USA). In Article III, soil temperature and SWC were recorded manually during each sampling session using a temperature probe (107, Campbell Scientific Inc., Logan, UT, USA) and a moisture sensor (ProCheck, Decagon Devices, Inc., Pullman, WA, USA).

## 1.5. Soil physiochemical parameters (Articles I, III and IV)

Soil physiochemical parameters were analysed from soil samples collected from 0–0.1, 0.1–0.2 and 0.2–0.4 m (Article I) or 0–0.1 m (Articles III and IV) belowground, adjacent to the soil chambers. Soil ammonium (NH<sub>4</sub>) and nitrate (NO<sub>3</sub>) were determined from a 2M KCl extract by flow injection analysis. Total N contents of air-dried samples were determined by a dry-combustion method on a varioMAX CNS elemental analyser (Elementar Analysensysteme GmbH, Germany). The soil organic matter content of dry matter was determined by loss on ignition at 550 °C. The physiochemical analyses were performed in the Estonian University of Life Sciences laboratory. The helium-atmosphere soil incubation method was used to measure potential N<sub>2</sub> fluxes from soil cores ex-situ (Butterbach-Bahl et al., 2002).

## 1.6. Soil microbial community abundance (Articles III and IV)

Soil microbial community abundances were quantified from soil samples collected 0–0.1 m belowground during the study periods for Articles III and IV. Soil samples were homogenised with lysis buffer using Precellys 24 Homogeniser (Berlin Technologies, Montigny-le-Bretonneux, France), followed by DNA extraction from 0.25 g of the soil sample using the DNeasy PowerSoil Pro kit (Qiagen, Hilden, Germany). The extracted DNA concentration and quality were determined using the Infinite M200 spectrophotometer (Tecan AG, Grodig, Austria). The abundance of bacterial and archaeal 16S rRNA genes were assessed with the Quantitative polymerase chain reaction (qPCR), using RotorGene® Q equipment (Qiagen, Valencia, CA, USA). Abundances of the following functional genes were determined: bacterial *amoA* (ammonia monooxygenase gene), archaeal *amoA*, COMAMMOX (complete ammonia oxidation), *nirK* (copper-containing nitrite reductase gene), *nirS* (cytochrome cd1-type nitrite reductase gene), *nosZ* I (clade I N<sub>2</sub>O reductase gene), and *nosZ* II (clade II N<sub>2</sub>O reductase

gene) for the N cycle, and *mcrA* (methyl coenzyme M reductase), *pmoA* (particulate methane monooxygenase) and *n-damo* (nitrate-dependent anaerobic methane oxidation) genes for the C cycle. Data processing was performed with the RotorGene Series Software (version 2.0.2, Qiagen, Hilden, Germany) and LinRegPCR program v. 2020.0. Analysis was conducted in the microbiology lab of the Department of Geography at the University of Tartu.

## 1.7. Xylem sap flow (Article I)

The xylem sap flow of birch and spruce trees was recorded with sap flow systems EMS81 (EMS Brno, Brno, Czech Republic) during the growing season. The sensors were mounted at 2–2.5 m from the ground level. The stem sap flow rate ( $\text{kg h}^{-1}$ ) was divided to stem xylem area ( $\text{cm}^2$ ) at the sensor height to calculate sap flux density ( $\text{g h}^{-1} \text{cm}^{-2}$ ).

## 1.8. Dissolved gas concentrations in birch sap and soil water (Article IV)

Dissolved  $\text{CH}_4$  and  $\text{CO}_2$  concentrations in birch sap ( $d\text{CH}_{4\text{sap}}$  and  $d\text{CO}_{2\text{sap}}$ ) were determined from sap samples collected in syringes connected to holes tapped into birch stems at 0.1 m and 1.7 m heights (Figure 2B). Dissolved gas concentrations in soil water ( $d\text{CH}_{4\text{soil}}$  and  $d\text{CO}_{2\text{soil}}$ ) were assessed from groundwater samples collected into syringes from groundwater wells. The water-atmosphere equilibration method was used, whereby 30 ml of ambient air was added to 30 ml of sap/water in the syringe and shaken for one minute. The equilibrated headspace air was then pushed to pre-evacuated vials, taken to the laboratory to be analysed for  $\text{CH}_4$  and  $\text{CO}_2$  concentrations using gas-chromatography. The dissolved gas concentrations were calculated as the sum of dissolved gas in the headspace and gas still dissolved in the water after shaking, according to equations based on Magen et al. (2014). The headspace gas concentrations in ppm were converted to gas amount ( $\mu\text{mol L}^{-1}$ ) using the ideal gas law at a temperature of sample extraction ( $10\text{ }^\circ\text{C}$ ).

## 1.9. Statistical analyses

Statistical analysis was performed using R version 4.0.3 (R core team, 2020). The Kolmogorov-Smirnov test was used to examine the normality of data distribution. Due to the non-normal distribution of flux data, non-parametric tests were employed. The significance of temporal variability of gas fluxes and differences between stem fluxes at different heights was determined using the Kruskal–Wallis one-way analysis of variance and Dunn’s multiple comparisons, corrected with the Bonferroni method, as a post hoc test. Spearman’s rank correlation and Principal Component Analysis (PCA) were employed to determine and visualise the significance and direction of relationships between the measured variables. A significance level of  $p < 0.05$  was used across all tests.

## 2. RESULTS AND DISCUSSION

### 2.1. Soil fluxes (Article I-IV)

#### 2.1.1. Quantification and temporal dynamics of soil fluxes

Soil fluxes of CH<sub>4</sub>, N<sub>2</sub>O and CO<sub>2</sub> were quantified, and their seasonal variations were determined. Different gases exhibited distinct seasonal patterns in their soil fluxes. Soil at the study site was a net annual sink of atmospheric CH<sub>4</sub> (Table 2; Figure 3B). The annual CH<sub>4</sub> uptake shown in Article I ( $-6.44 \pm 0.21 \mu\text{g C m}^{-2} \text{ h}^{-1}$ ) is marginally lower than previous findings in boreal forestry-drained peatlands (Korkiakoski et al., 2017; Lohila et al., 2011; Ojanen et al., 2010), being more similar to results from a nearby riparian forest (Mander et al., 2022). However, direct comparison with previous studies is challenging due to different measurement frequencies (Lohila et al., 2011) and interpolation of fluxes from only a few measurement occasions (Ojanen et al., 2010).

The seasonal dynamics of soil CH<sub>4</sub> fluxes agreed with previous results from boreal drained peatland forests (Korkiakoski et al., 2017; Lohila et al., 2011; Ojanen et al., 2010), characterised by minor uptake during winter-onset, near-zero fluctuations in the dormant season and substantial uptake in the summer months, peaking in late-July (Figure 3B). During winter, snow cover can impede gas exchange and the ice in soil pores of the frozen topsoil could restrict gas diffusion (Borken et al., 2006). Changes in pressure during spring freeze-thaw periods can release CH<sub>4</sub> stored in frozen soils into the atmosphere (Kim et al., 2012). In addition, methanogenesis is facilitated when the melting of the snow and ice creates anaerobic conditions in the soil. In the studied drained peatland forest, the near-zero fluctuations of CH<sub>4</sub> in the dormant season imply a balance between methanogenesis and methanotrophy in the soil. As the site was not submerged, i.e. WTD stayed belowground (Figure 3A), there was always a layer of the soil where aerobic methanotrophy counteracted the CH<sub>4</sub> production in deeper soil layers with anaerobic conditions. In the summer, the soil turned into a substantial CH<sub>4</sub> sink as temperature increased and WTD markedly decreased. This has also been evidenced in boreal drained peatland forests, although the beginning and end of the continuous CH<sub>4</sub> sink period in the growing season varied.

Table 2. Average (mean  $\pm$  SE) fluxes of CH<sub>4</sub> ( $\mu\text{g C m}^{-2} \text{h}^{-1}$ ), N<sub>2</sub>O ( $\mu\text{g N m}^{-2} \text{h}^{-1}$ ) and CO<sub>2</sub> ( $\text{mg C m}^{-2} \text{h}^{-1}$ ) from soil, birch stems and spruce stems, averaged for the full measurement period (October 2020–October 2021 for stem fluxes and December 2020–August 2021 for soil fluxes), the wetter period (22 October 2020–12 July 2021) and the drier period (13 July 2021–20 October 2021 for stem fluxes and 13 July 2021–19 August 2021 for soil fluxes) (Article I), and the winter period (22 October 2020–3 May 2021, Article II). The drier period was defined by the site-average SWC being continuously  $< 0.3 \text{ m}^3 \text{ m}^{-3}$  (Article I).

	CH <sub>4</sub> ( $\mu\text{g C m}^{-2} \text{h}^{-1}$ )	N <sub>2</sub> O ( $\mu\text{g N m}^{-2} \text{h}^{-1}$ )	CO <sub>2</sub> ( $\text{mg C m}^{-2} \text{h}^{-1}$ )
<b><i>Full period</i></b>			
Soil	$-6.44 \pm 0.21$	$42.4 \pm 1.8$	$43.1 \pm 1.5$
Birch	$1.12 \pm 0.12$	$2.50 \pm 0.38$	$92.1 \pm 3.2$
Spruce	$0.231 \pm 0.050$	$-0.242 \pm 0.031$	$61.4 \pm 2.1$
<b><i>Wetter period</i></b>			
Soil	$-3.04 \pm 0.18$	$43.6 \pm 2.0$	$26.9 \pm 1.1$
Birch	$1.40 \pm 0.16$	$3.28 \pm 0.49$	$79.9 \pm 3.8$
Spruce	$0.226 \pm 0.072$	$-0.107 \pm 0.035$	$54.7 \pm 52.49$
<b><i>Drier period</i></b>			
Soil	$-32.2 \pm 1.2$	$33.4 \pm 3.0$	$165.0 \pm 6.5$
Birch	$0.353 \pm 0.077$	$0.308 \pm 0.387$	$126.0 \pm 5.7$
Spruce	$0.244 \pm 0.083$	$-0.62 \pm 0.06$	$80.1 \pm 3.9$
<b><i>Winter</i></b>			
Soil	$-2.00 \pm 0.12$	$50.46 \pm 2.77$	–
Birch	$0.18 \pm 0.03$	$1.44 \pm 0.22$	–
Spruce	$0.10 \pm 0.03$	$0.003 \pm 0.01$	–

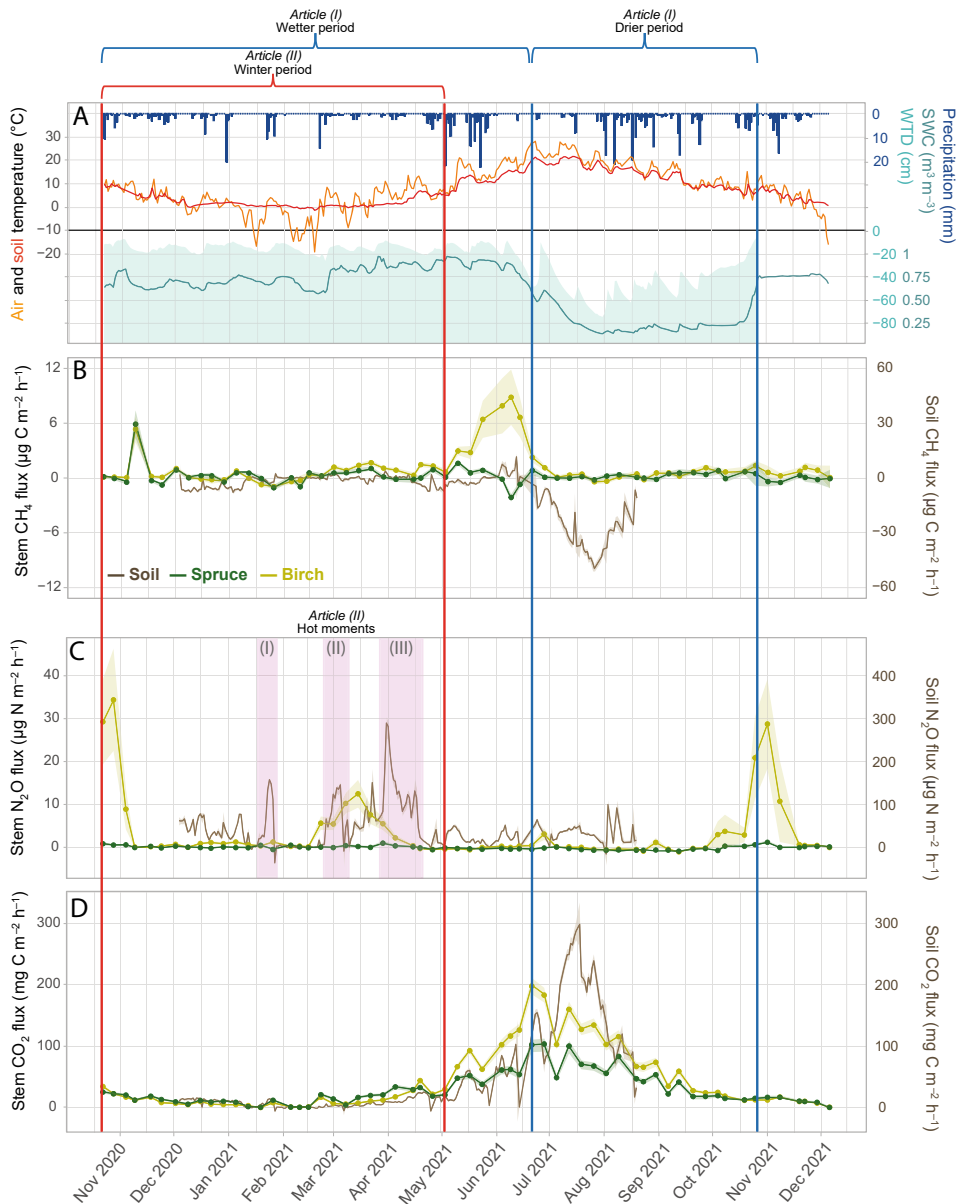


Figure 3. Temporal dynamics of soil and stem  $\text{CH}_4$ ,  $\text{N}_2\text{O}$  and  $\text{CO}_2$  fluxes and environmental variables in the drained peatland forest. **(A)** Daily mean air and soil temperatures ( $^{\circ}\text{C}$ ), soil water content (SWC,  $\text{m}^3 \text{m}^{-3}$ ), water table depth (WTD, cm), and daily sum precipitation (mm) (October 2020–December 2021); daily mean soil (December 2020–August 2021) and stem (October 2020–December 2021) **(B)**  $\text{CH}_4$  ( $\mu\text{g C m}^{-2} \text{h}^{-1}$ ), **(C)**  $\text{N}_2\text{O}$  ( $\mu\text{g N m}^{-2} \text{h}^{-1}$ ) and **(D)**  $\text{CO}_2$  ( $\text{mg C m}^{-2} \text{h}^{-1}$ ) fluxes with standard error as the shaded area. Stem fluxes are expressed in units per  $\text{m}^2$  of stem surface area. Soil fluxes are expressed in units per  $\text{m}^2$  of soil surface area. Blue vertical lines emphasise drier and wetter periods of the year. The drier period was defined by SWC being continuously  $< 0.3 \text{ m}^3 \text{m}^{-3}$ . Drier period: 13 July 2021–20 October 2021; wetter period: 22 October 2020–12 July 2021 (Article I). The winter period (Article II study period) has been marked with red vertical lines. Hot moments of soil  $\text{N}_2\text{O}$  fluxes are emphasised by pink shaded areas: (I) 20/01/2021–27/01/2021, (II) 22/02/2021–09/03/2021, and (III) 27/03/2021–20/04/2021 (Article II).

Three hot moments were identified in Article II: (I) 20/01/2021–27/01/2021, (II) 22/02/2021–09/03/2021, and (III) 27/03/2021–20/04/2021 (Figure 3C). Hot moments are known to determine temporal dynamics of N<sub>2</sub>O emissions from soils (Barrat et al., 2021; Mander et al., 2021). They are primarily induced by changes in SWC, for example, during freeze-thaw cycles (Groffman et al., 2006; Teepe et al., 2001). Hot moments (I) and (II) likely resulted from soil freeze-thaw events, as increases in N<sub>2</sub>O emissions coincided with rising WTD, SWC and air temperature in winter and spring (Figure 3A; 3C). Soil freeze-thaw events affect N<sub>2</sub>O release through several mechanisms. Dead cells of microorganisms, fine roots, and mycorrhiza frozen in the soil, can rapidly decompose during thawing (Groffman et al., 2006; Teepe et al., 2001). While fine roots die and start to decompose, they can also reduce competition for inorganic N, leaving more NO<sub>3</sub> available for microorganisms for N<sub>2</sub>O production through denitrification (Groffman et al., 2006). In addition, nitrifier denitrification has been shown to dominate total denitrification in fluctuating aerobic-anaerobic conditions in low temperatures (Ma et al., 2007), in part as increased oxygen content in snow melt water can inhibit the full denitrification pathway, leading to increased N<sub>2</sub>O production (Öquist et al., 2004). Hot moment (III) exhibited the highest N<sub>2</sub>O emissions, driven by a combination of fluctuations in SWC and rising air and soil temperatures. After reaching optimal SWC conditions for N<sub>2</sub>O production in the soil, temperature increase further stimulates microbial activity, driving the N<sub>2</sub>O peak (Mander et al., 2021). The significance of hot moments in temporal soil N<sub>2</sub>O dynamics emphasises that focusing solely on average flux values over a study period may be inadequate. Models interpolating snapshot fluxes must incorporate these peaks to accurately represent N<sub>2</sub>O dynamics.

Soil CO<sub>2</sub> fluxes presented in this study refer to forest floor respiration, encompassing heterotrophic respiration in the soil and autotrophic respiration occurring from plants inside the measurement chamber and belowground from plant roots and the associated mycorrhizal fungi. The results of annual forest floor respiration ( $43.1 \pm 1.5 \text{ mg C m}^{-2} \text{ h}^{-1}$ ; Table 2; Figure 3D) were lower than previous results on respiration measured with the chamber method (Maljanen et al., 2010; Ojanen et al., 2010). Soil CO<sub>2</sub> efflux followed a seasonal trend of near-zero fluxes during the dormant season and increased fluxes during the growing season (Figure 3D), widely reported by previous studies (Järveoja et al., 2018; Maljanen et al., 2010; Minkkinen et al., 2007). Respiration increased in spring and peaked in mid-July (maximum daily average  $297 \pm 35.8 \text{ } \mu\text{g C m}^{-2} \text{ h}^{-1}$ ), after which emissions decreased again towards the end of summer (Figure 3D).

### 2.1.2. Environmental drivers of soil fluxes

On an annual scale, soil hydrological variables were the strongest positive drivers of soil CH<sub>4</sub> fluxes with higher WTD and SWC reducing CH<sub>4</sub> uptake and increasing emissions, whereas soil and air temperature had negative relationships with fluxes, as higher temperatures correspond to enhanced CH<sub>4</sub> uptake (Table 3; Figure 4; Article I). These relationships persisted in the winter period but were not as strong (Article II). However, during springtime (Article IV), temperature was the primary driver of soil fluxes and hydrological factors had no significant

effects. These disparities suggest that soil hydrological variables SWC and WTD play a stronger role in soil CH<sub>4</sub> flux dynamics in the long term, significantly influencing budgets over the year or between wetter and drier periods (Article I). However, over shorter periods, e.g. in spring (Article IV), air and soil temperatures become more direct governing factors of the fluxes. Similarly, while annual trends of soil N<sub>2</sub>O fluxes and related environmental variables may be distorted by the hot moments described above, analysis of the springtime drivers revealed that when SWC was in optimum range for N<sub>2</sub>O production, temperature became the primary driver of fluxes. Forest floor CO<sub>2</sub> fluxes had strong positive correlations with air and soil temperatures on all measured timescales, relating to the growing season and plant physiological activity, influenced by the temperature sensitivity of respiration and diffusion rates (Teskey et al., 2008) (Table 3; Figure 4; Articles I and IV).

Table 3. Spearman's correlations between birch, spruce and soil CH<sub>4</sub>, N<sub>2</sub>O and CO<sub>2</sub> fluxes, and soil environmental variables, as well as chemical parameters from the topsoil layer (0–0.1 m) during the annual measurement period (Article I). Statistically significant correlations have been marked in bold ( $p < 0.05$ ).

	CH <sub>4</sub> ( $\mu\text{g C m}^{-2} \text{h}^{-1}$ )			N <sub>2</sub> O ( $\mu\text{g N m}^{-2} \text{h}^{-1}$ )			CO <sub>2</sub> ( $\text{mg C m}^{-2} \text{h}^{-1}$ )		
	Birch	Spruce	Soil	Birch	Spruce	Soil	Birch	Spruce	Soil
Soil water content ( $\text{m}^3\text{m}^{-3}$ )	<b>0.18</b>	-0.03	<b>0.47</b>	<b>0.21</b>	<b>0.23</b>	-0.03	<b>-0.23</b>	-0.07	<b>-0.38</b>
Water table depth (cm)	<b>0.11</b>	-0.02	<b>0.52</b>	<b>0.39</b>	<b>0.41</b>	-0.02	<b>-0.52</b>	<b>-0.40</b>	<b>-0.51</b>
Soil temperature (°C)	<b>0.15</b>	-0.06	<b>-0.46</b>	<b>-0.33</b>	<b>-0.37</b>	<b>0.15</b>	<b>0.88</b>	<b>0.73</b>	<b>0.81</b>
Air temperature (°C)	0.26	-0.15	<b>-0.35</b>	<b>-0.37</b>	<b>-0.54</b>	<b>0.16</b>	<b>0.95</b>	<b>0.94</b>	<b>0.87</b>
Stem temperature (°C) <sup>1</sup>	-0.04	<b>0.37</b>		<b>0.53</b>	0.19		<b>0.61</b>	<b>0.54</b>	
NH <sub>4</sub> <sup>+</sup> (mg N/kg)	<b>0.27</b>	0.08	0.08	0.14	-0.01	0.18	<b>0.20</b>	0.19	<b>0.32</b>
NO <sub>3</sub> <sup>-</sup> (mg N/kg)	<b>-0.40</b>	-0.04	<b>-0.37</b>	<b>-0.17</b>	0.06	0.04	<b>-0.18</b>	-0.21	0.01
Soil N <sub>2</sub> flux ( $\mu\text{g N m}^{-2} \text{h}^{-1}$ )	<b>0.29</b>	<b>0.31</b>	<b>0.22</b>	0.01	0.10	-0.11	0.15	0.04	-0.02
Sap flow density ( $\text{g/h/cm}^2$ ) <sup>1</sup>	-0.01	-0.20		<b>0.38</b>	0.31		<b>0.56</b>	0.28	
Soil CH <sub>4</sub> flux ( $\mu\text{g C m}^{-2} \text{h}^{-1}$ )	<b>0.24</b>	0.10	<i>I</i>	<b>0.18</b>	<b>0.21</b>	<b>-0.26</b>	<b>-0.36</b>	<b>-0.34</b>	<b>-0.56</b>
Soil N <sub>2</sub> O flux ( $\mu\text{g N m}^{-2} \text{h}^{-1}$ )	-0.02	-0.03	<b>-0.26</b>	<b>0.18</b>	0.04	<i>I</i>	<b>0.16</b>	0.09	<b>0.37</b>
Soil CO <sub>2</sub> flux ( $\text{mg C m}^{-2} \text{h}^{-1}$ )	0.07	-0.11	<b>-0.56</b>	<b>-0.31</b>	<b>-0.29</b>	<b>0.37</b>	<b>0.76</b>	<b>0.64</b>	<i>I</i>

<sup>1</sup> Note that sap flow and stem temperature were only measured during the growing season (29 May–10 September 2021). The presented correlations are based on stem flux data corresponding to this period.

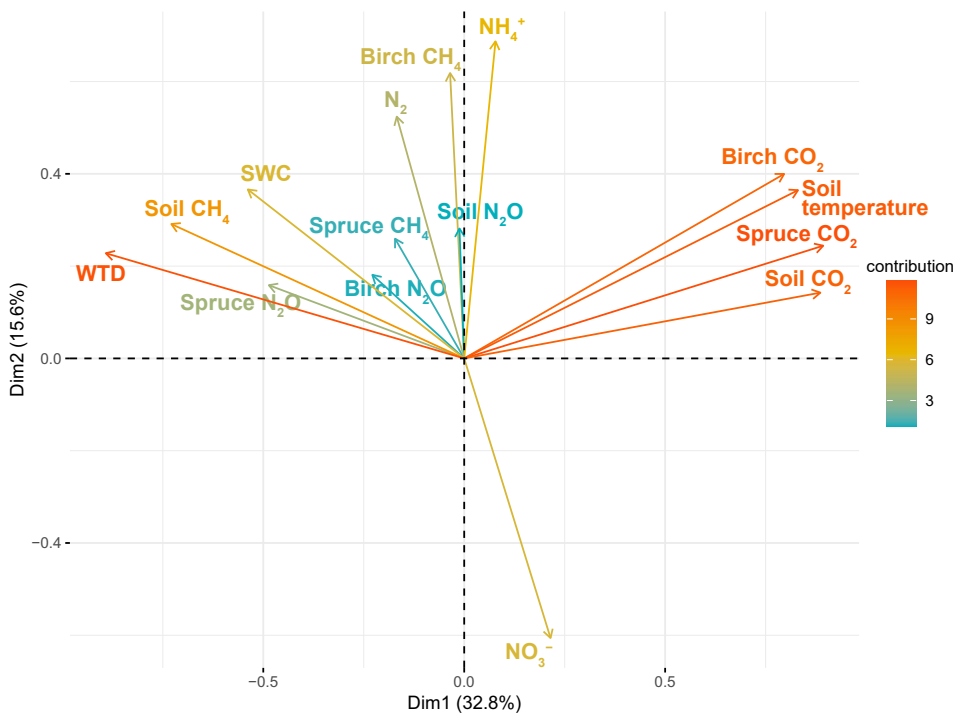


Figure 4. Principal Component Analysis of the annual birch, spruce and soil CH<sub>4</sub>, N<sub>2</sub>O and CO<sub>2</sub> fluxes and soil environmental and chemical parameters. Abbreviations: WTD – water table depth, SWC – soil water content. Note that the PCA was performed using monthly averages of soil and stem fluxes and environmental variables from all 12 measuring points to enable comparison with soil chemical parameters, analysed from soil samples collected once a month (n=144) (Article I).

### 2.1.3. Effects of soil thawing on N<sub>2</sub>O fluxes

As the significance of hot moments in temporal soil N<sub>2</sub>O emissions' dynamics has been shown by previous research in an adjacent riparian forest (Mander et al., 2021), as well as by the results from Article II, a soil heating experiment was conducted to further unravel N<sub>2</sub>O emission processes during freeze-thaw events (Article III). The aim of the experiment was to assess the effects of freezing and thawing on N<sub>2</sub>O fluxes, SWC, and microbial communities in the soil. The heating in the soil collars induced a significant increase in soil temperature and SWC, initiating the thawing of the topsoil layer. N<sub>2</sub>O emissions increased during the heating sessions together with SWC, displaying a significant positive correlation with SWC. Mean N<sub>2</sub>O emissions on three measurement days increased from 72.9  $\mu\text{g N m}^{-2} \text{h}^{-1}$  in S1, to 107  $\mu\text{g N m}^{-2} \text{h}^{-1}$  in S2 and 128.5  $\mu\text{g N m}^{-2} \text{h}^{-1}$  in S3, with statistically significant differences between S1 and S3 on all days (Figure 5). The mean N<sub>2</sub>O flux after induced thawing corresponds to hot moments I and II observed in Article II. Soil N<sub>2</sub>O emissions peaked at 0.5–0.7 m<sup>3</sup> m<sup>-3</sup> SWC, which is lower than for the hot moments in Article II, but in the same range as previously

reported for N<sub>2</sub>O emissions during thawing (Teepe et al., 2004). Meltwater-induced increases in SWC affect the availability of oxygen and enhance microbial activity in the soil, activating the soil N substrate (Wagner-Riddle et al., 2008; Wang et al., 2023).

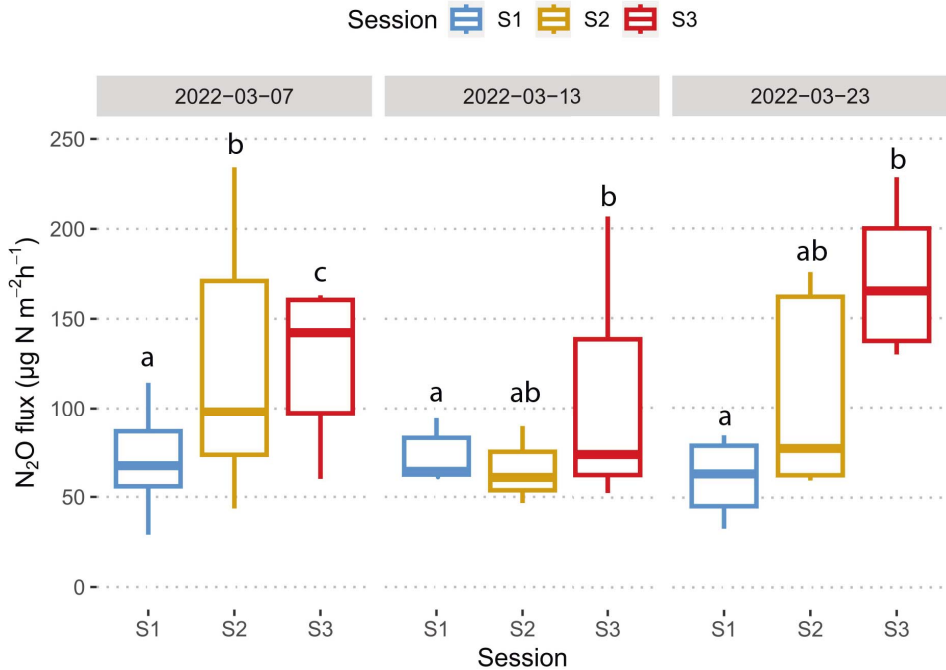


Figure 5. Soil N<sub>2</sub>O emissions during sampling sessions on different measurement days of the freeze-thaw experiment. S1 is the session without heating, S2 is the first session with heating on, and S3 is the session with prolonged heating. Boxplots are based on 9 measurements (n=9) in each session on 07/03/2022, and 5 measurements (n=5) in each session on 13/03/2022 and 23/03/2022. The box in the boxplot indicates the data points between the 25th and 75th percentile, whiskers show the range of all data points excluding the outliers., and the intersected line in the box represents the median. Different letters above bars indicate statistically significant differences between fluxes during different sessions on each measurement day, according to ANOVA, followed by Games-Howell post-hoc test (p<0.05). (Article III)

#### 2.1.4. Soil chemistry and microbial community composition

Soil nutrient availability plays a crucial role in regulating peatland GHG fluxes (Korkiakoski et al., 2017; Lohila et al., 2011), providing labile substrate to soil microbes (Wu et al., 2020). Examining changes in the soil inorganic N (NO<sub>3</sub> and NH<sub>4</sub>) pool alongside variations in soil microbial abundances helps disentangle the microbial processes governing GHG production and consumption in the soil, particularly CH<sub>4</sub> and N<sub>2</sub>O.

In both the annual study (Article I) and springtime investigation (Article IV), soil  $\text{NO}_3^-$  and  $\text{NH}_4^+$  contents exhibited opposing temporal patterns (Figure 6; Article IV Figure 3). Despite the absence of significant correlations between soil  $\text{NO}_3^-$  contents and  $\text{N}_2\text{O}$  emissions on an annual scale, soil  $\text{NO}_3^-$  increased directly before the springtime hot moment of  $\text{N}_2\text{O}$  emissions (Figure 6; Figure 3C). Rapid decomposition during thawing may have increased  $\text{NO}_3^-$  availability, and rising SWC consequently amplified the reduction of this  $\text{NO}_3^-$  to  $\text{N}_2\text{O}$  through denitrification under anaerobic soil conditions (Groffman et al., 2006; Teepe et al., 2001). In the springtime study (Article IV), soil  $\text{NO}_3^-$  content displayed similar temporal trends to GHG flux dynamics, however correlations with soil gas fluxes were only significant for  $\text{CO}_2$ , likely as an indirect relationship through air temperature and photosynthetically active radiation (PAR).

Soil  $\text{NH}_4^+$  content over the full year was driven by soil temperature and correlated positively with soil  $\text{CO}_2$  fluxes. This suggests that N mineralisation and organic matter decomposition processes, which contribute to soil  $\text{NH}_4^+$  content, are stimulated under warmer conditions (Groffman et al., 2006). Although no significant relationship emerged between  $\text{NH}_4^+$  content and soil  $\text{CH}_4$  fluxes, temporal dynamics illustrated that periods of increased  $\text{NH}_4^+$  in the soil coincided with greater  $\text{CH}_4$  uptake during the drier period (Figure 6; Figure 3B). Under aerobic soil conditions, soil N availability has been shown to enhance the growth and activity of methanotrophs, increasing  $\text{CH}_4$  uptake (Aronson & Helliker, 2010; Bodelier & Laanbroek, 2004). Conversely, during springtime,  $\text{NH}_4^+$  content was highest at the beginning of the study period and was consumed in the topsoil as spring progressed (Article IV Figure 3).  $\text{NH}_4^+$  can enter the soil during early spring from the decomposition of thawing plant residues and dead microorganisms frozen in the soil (Groffman et al., 2006; Ueda et al., 2015). The  $\text{NH}_4^+$  content is reduced alongside declining WTD and SWC, suggesting that nitrification occurs in the soil as more aerobic conditions prevail. This was further evidenced by increasing  $\text{NO}_3^-$  content, a product of nitrification.

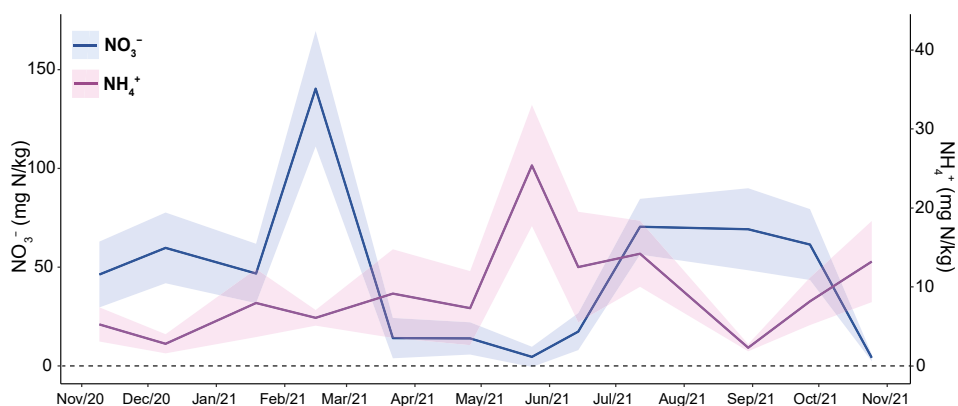


Figure 6. Average soil ammonium ( $\text{NH}_4^+$ ) and nitrate ( $\text{NO}_3^-$ ) (mg N/kg) determined from topsoil (0–0.1 m) samples once a month across the annual study period (November 2020–October 2021; Article I). Note the secondary axis for  $\text{NH}_4^+$ -N. The shaded area marks the 95% confidence intervals of measurements.

The abundance of soil microbial communities responsible for different processes in the N and C cycles offers insights into the genetic potential for GHG production and release. During the freeze-thaw experiment (Article III), nitrification likely drove the initial N<sub>2</sub>O production in the thawing soil. This was evidenced by an increase in bacterial nitrifiers, consumption of NH<sub>4</sub> and an increase in NO<sub>3</sub> during the onset of thawing. The initial topsoil thawing created aerobic soil conditions for nitrifiers to thrive. However, the increasing SWC during prolonged heating sessions resulted in anaerobic conditions and a decline in bacterial nitrifiers' abundance. Abundances of nitrifying genes archaeal *amoA* and COM-AMMOX kept increasing with heating sessions and peaked at the elevated SWC conditions, possibly related to the resilience of ammonia-oxidising archaea in prolonged anoxic conditions (Pett-Ridge et al., 2013). The abundance of denitrifying *nirK* and *nirS* genes also increased as a result of thawing, aligning with previous findings (Smith et al., 2010). Furthermore, positive correlations occurred between soil N<sub>2</sub>O fluxes and ratios of N<sub>2</sub>O producers to reducers (*nir/nosZ*) and denitrification genes to nitrification genes (*nir/amoA*). The results revealed the predominance of *nirK* gene abundance over *nirS* in the total *nir* gene pool. Higher soil N<sub>2</sub>O production has been shown in ecosystems with such *nir* gene relationships. This is due to the co-occurrence of *nirS* and N<sub>2</sub>O-reducing *nosZ* genes in denitrifying microorganisms, meaning that *nirS*-containing microbes are more capable of complete denitrification (Espenberg et al., 2018; Graf et al., 2014). The significance of *nirK*-based denitrifiers in N<sub>2</sub>O production was further emphasised by positive correlations between N<sub>2</sub>O fluxes and the abundance of *nirK* genes.

Abundances of the *nosZ* gene did not significantly change in response to the increase in SWC during the experiment. Although these N<sub>2</sub>O reductase genes favour anaerobic environments to be able to consume N<sub>2</sub>O (Wang et al., 2022), sufficient anaerobic conditions may not have been achieved with thawing in this study. Furthermore, decreased abundances of N<sub>2</sub>O reducers have been reported at soil temperatures below 5 °C, resulting in an increase in N<sub>2</sub>O fluxes, while N<sub>2</sub>O-producing denitrifiers remain unaffected by the low temperatures (Wagner-Riddle et al., 2010). Soil temperatures during the experiment did not exceed 4 °C, remaining too low for the *nosZ*-type denitrifiers to show their enhanced N<sub>2</sub>O reduction capacity.

While nitrification was initiated at the beginning of the warming, incomplete denitrification was the main driver of the increased soil N<sub>2</sub>O emissions. This aligns with previous studies highlighting the importance of denitrification in driving rapid N<sub>2</sub>O emissions peaks during freeze-thaw events (Smith et al., 2010; Wagner-Riddle et al., 2008). The results support rewetting drained peatland forests as a promising mitigation strategy to reduce N<sub>2</sub>O emissions. Elevated and more stable water levels can help maintain favourable temperatures for N<sub>2</sub>O-reducing *nosZ*-type denitrifiers in the soil microbiome, promoting complete denitrification processes.

The springtime study period (Article IV) reflected conditions following the freeze-thaw cycle, characterised by elevated SWC and WTD that gradually decrease (Article IV Figure 1). Significant changes in the abundances of various

functional genes between measurement days were observed, with different genes dominating the variability of observations across days for both the N and C cycles (Article IV Figure 6). The abundances of N<sub>2</sub>O reductase *nosZ* I and II genes were elevated at lower soil temperatures early in the study period, coinciding with high WTD and SWC, suggesting genetic potential for complete denitrification under these conditions. However, nitrification processes were also evident. As temperatures rose and WTD and SWC began declining, NH<sub>4</sub> levels decreased and NO<sub>3</sub> increased. This indicates that nitrification processes were initiated in the soil, converting NH<sub>4</sub> to NO<sub>3</sub>. Thus, both nitrification and complete denitrification were evident, with nitrification responsible for the low, but observable, N<sub>2</sub>O emissions at the beginning of the spring study period. After the soil NO<sub>3</sub> content peak at the end of April, NO<sub>3</sub> levels declined, likely as it started to be converted to N<sub>2</sub>O through incomplete denitrification by *nirK* and *nirS* genes. This was evidenced by high *nir* gene abundance and a high *nir/nosZ* ratio in the middle of the measurement period (Article IV Figure 4). In May, the NO<sub>3</sub> pool was depleted and N<sub>2</sub>O emissions decreased. However, a high N<sub>2</sub>O reductase (*nosZ*) gene abundance was not observed at the end of the study period to confirm the decline in emissions.

Furthermore, in Article IV, the genetic composition influencing the C cycle was explored, particularly methanogenesis and methanotrophy. A gradual decrease in methanogenic potential and an increase in methanotrophic potential occurred, indicated by the declining methanogenic-to-methanotrophic gene ratio over the measurement period. On the second measurement day, n-damo was driving the methanotrophic abundance, switching to the *pmoA* gene dominance by the end of the study (Article IV Figure 5). The gene ratio negatively correlated with soil CO<sub>2</sub> fluxes, possibly due to CH<sub>4</sub> being oxidised to CO<sub>2</sub> (Hu et al., 2014). However, only the n-damo genetic abundance correlated with soil CH<sub>4</sub> fluxes, and this relationship was positive, although n-damo is generally responsible for CH<sub>4</sub> consumption in the aerobic-anaerobic interface under high levels of nitrate (Hu et al., 2014; Zhou et al., 2014). This indicates the need for a more detailed analysis of the relationships between C cycle genes and fluxes under different environmental conditions.

## 2.2. Tree stem fluxes (Article I, II, IV)

### 2.2.1. Quantification and temporal dynamics of stem fluxes

The first account of annual measurements of tree stem GHG fluxes in a drained peatland forest was provided in Article I. Notably, the cold period has been largely overlooked in stem flux studies across different ecosystems. Tree stems were a net annual source of CH<sub>4</sub>, with higher emissions from birch stems than from spruce stems (Table 2; Figure 3B). Previous studies in wetlands have reported higher annual stem CH<sub>4</sub> flux values from various broadleaved tree species (Jeffrey et al., 2023a; Moldaschl et al., 2021; Pangala et al., 2015). However, long-term measurements from forests with drier conditions, which could be more comparable to the drained forest investigated here, are lacking. The temporal

dynamics of tree stem CH<sub>4</sub> fluxes exhibited near-zero fluctuations for most of the year, with isolated emissions' peaks in autumn and summer (Figure 3B). Both birch and spruce stem emissions increased in November, coinciding with an increase in SWC. In spring, birch and spruce stems were minor CH<sub>4</sub> sources, following the rising water table after snowmelt. This pattern was also observed in the spring-time study (Article IV Figure 1) and documented in a temperate wetland forest (Pangala et al., 2015). The most pronounced peak in birch stem CH<sub>4</sub> emissions occurred in late June, with daily mean values reaching  $8.47 \pm 3.14 \mu\text{g C m}^{-2} \text{h}^{-1}$ . This peak coincided with the end of the wetter period, where sustained higher water levels and increasing soil temperatures likely created optimal conditions for methanogenesis in the soil (Figure 3A; 3B) (Pangala et al., 2015; Pitz & Magonigal, 2017). This summer peak was not observed for spruce stem CH<sub>4</sub> fluxes. On average, stems emitted more CH<sub>4</sub> during the wetter period of the year, primarily driven by the peaks.

Birch stems were net annual emitters of N<sub>2</sub>O, whereas spruce stems exhibited minor N<sub>2</sub>O uptake (Table 2; Figure 3C). Birch N<sub>2</sub>O emissions observed in this study exceeded those from birch and spruce trees in a boreal forest (Machacova et al., 2019), alder trees in a hemiboreal riparian forest (Mander et al., 2021), and ash and poplar in a temperate floodplain forest (Moldaschl et al., 2021). The N<sub>2</sub>O consumption observed in spruce stems has previously only been reported for broadleaved tree species in temperate upland forests during the growing season (Barba et al., 2019b; Machacova et al., 2017). This uptake has been shown to be related to a concentration gradient where atmospheric N<sub>2</sub>O concentrations exceed those in the stem (Barba et al., 2019b), or to the presence of cryptogamic stem covers (Machacova et al., 2017), which were not, however, evident on the measured spruce trees. Birch stems emitted N<sub>2</sub>O throughout the year, with notable peaks in autumn and spring (Figure 3C). The highest daily average emissions were recorded in autumn, reaching  $34.3 \pm 11.9 \mu\text{g N m}^{-2} \text{h}^{-1}$  in October 2020 and  $28.7 \pm 0.455 \mu\text{g N m}^{-2} \text{h}^{-1}$  in November 2021. A smaller peak was observed in early spring (Figure 3C). This springtime peak coincided with the hot moments of soil N<sub>2</sub>O release. The freeze-thaw related N<sub>2</sub>O production processes in the soil, as discussed in previous chapters, likely increased N<sub>2</sub>O readily available to be taken up by tree roots, leading to elevated stem emissions. However, no soil flux data is available for comparison with autumn stem flux peaks. Emissions during these peak periods accounted for 94.9% of the cumulative annual birch stem flux. Early autumn and early spring also contributed most to the cumulative stem N<sub>2</sub>O emissions from alder in a riparian forest (Mander et al., 2021). In contrast, spruce stem fluxes were negligible and fluctuated around zero throughout the year, differing from findings in a boreal forest, where higher emissions from spruce than from birch stems were observed throughout the year (Machacova et al., 2019).

Both birch and spruce stems had a positive CO<sub>2</sub> flux throughout the year (Table 2; Figure 3D). Annual measurements of stem CO<sub>2</sub> fluxes were approximately 10 times higher than those observed from European beech in a temperate upland forest (Machacova et al., 2023) and from Scots pine in a boreal forest (Kolari et al., 2009). Temporal dynamics of stem CO<sub>2</sub> efflux followed a seasonal

trend, with low fluxes during the dormant season and a gradual increase during spring months (Figure 3D). This was also observed in the springtime study (Article IV Figure 1). Fluxes peaked at the end of June, with daily averages reaching  $394.9 \pm 26.7 \text{ mg C m}^{-2} \text{ h}^{-1}$  for birch and  $206.3 \pm 24.8 \text{ mg C m}^{-2} \text{ h}^{-1}$  for spruce. This was followed by a gradual decrease of fluxes towards autumn (Figure 3D). Stem  $\text{CO}_2$  flux trends coinciding with tree growth phenology have also been observed in Norway spruce at a subalpine site (Etzold et al., 2013), Scots pine in a boreal forest (Kolari et al., 2009) and European beech in a temperate upland (Machacova et al., 2023). In contrast to  $\text{CH}_4$  and  $\text{N}_2\text{O}$  dynamics, average stem  $\text{CO}_2$  release was higher during the drier period (Table 2), driven by the temperature sensitivity of plant respiration and diffusion rates (Teskey et al., 2008).

The inter-species variance in temporal stem flux patterns highlights the need to contextualise the processes driving GHG fluxes according to tree species. Flux variations can be caused by site-level differences in microtopography, creating variations in SWC and WTD. Thus, trees growing in depressions with higher water availability may emit more  $\text{CH}_4$  and  $\text{N}_2\text{O}$  (Jeffrey et al., 2020; Terazawa et al., 2015). Birch trees, which are better adapted to wetter conditions than spruces, may prefer such locations as their habitat in the forest (Kozłowski, 1997). In addition, the spatial variability of gas concentrations in the soil water can influence the quantities of dissolved gases transported up the xylem (Machacova et al., 2016; Machacova et al., 2019). Root depth and density also vary between tree species. Spruces generally exhibit higher fine root density closer to the soil surface, whereas birch roots reach deeper soil layers to facilitate water uptake and gas transport, particularly for  $\text{CH}_4$  that may originate from deeper methanogenic soil layers (Puhe, 2003). Furthermore, stem morphology and tree physiology differ between broadleaved and coniferous trees, leading to variations in transpiration and gas diffusion rates (Pitz & Megonigal, 2017; Salomón et al., 2016; Teskey et al., 2008). While conifers generally have lower wood density, which might suggest higher GHG fluxes due to enhanced radial diffusion (Machacova et al., 2019; Zhang et al., 2020), the results show birch emissions surpassing spruce fluxes for all gases. This pattern aligns with findings from a boreal forested fen (Vainio et al., 2022). Furthermore, differences in xylem structures can affect sap flow rates. Conifers use tracheids for water transport within the xylem, while broadleaved trees have wider vessels, facilitating more efficient water transport (Zhang et al., 2020). Higher sap flow rates were also observed in birch in Article I (Figure 7). Additionally, birch trees exhibit paper-like bark layers, favourable for potential axial bark-mediated gas diffusion, as demonstrated in lowland *Melaleuca quinquenervia* trees (Jeffrey et al., 2023a). However, more studies are needed to understand how wood and bark anatomy influence stem GHG fluxes and how species-specific tree physiological traits affect gas transport in the soil-tree-atmosphere continuum.

### 2.2.2. Environmental drivers of stem fluxes

Across the annual study period, birch stem CH<sub>4</sub> fluxes were primarily driven by changes in soil hydrological conditions and temperature, positively correlating with SWC, soil temperature and WTD (Table 3). Higher SWC and WTD are commonly associated with higher stem CH<sub>4</sub> emissions, providing anaerobic conditions needed for methanogenesis in the soil, resulting in more CH<sub>4</sub> available for uptake by tree roots (Barba et al., 2019a; Barba et al., 2024). Conversely, spruce CH<sub>4</sub> fluxes did not exhibit significant correlations with any measured environmental variables on an annual scale (Table 3). In the springtime study (Article IV), the relationships between stem CH<sub>4</sub> fluxes and soil hydrological variables were negative, while air temperature and PAR were positive drivers. These opposing results suggest that soil hydrological conditions may play a greater role in CH<sub>4</sub> flux dynamics in the long term, such as with transitions between dry and wet periods, rather than being direct short-term governing factors. For birch trees, which have low-reaching rooting systems (Bachofen et al., 2024), this may be due to stem-emitted CH<sub>4</sub> originating from deeper soil layers where methanogenesis prevails, as it is absorbed by tree roots and transported up the xylem. Consequently, changes in WTD and SWC in the topsoil layers have a less pronounced impact on stem CH<sub>4</sub> emissions (Pangala et al., 2015). Birch CH<sub>4</sub> fluxes also had a negative correlation with soil NO<sub>3</sub> content, and positive relationships with NH<sub>4</sub> content and soil N<sub>2</sub> flux, while spruce CH<sub>4</sub> correlated positively with N<sub>2</sub> flux (Table 3). It is likely that these observed relationships are also linked to changes in soil hydrology, as anaerobic conditions lead to reduction of NO<sub>3</sub> and production of N<sub>2</sub> through denitrification. Results from Article IV also suggested that CH<sub>4</sub> emissions from birch stems were influenced by soil NH<sub>4</sub> and NO<sub>3</sub> levels. However, the relationships were reversed, with birch stems releasing more CH<sub>4</sub> when NH<sub>4</sub> content in the topsoil was low, likely due to NH<sub>4</sub> conversion to NO<sub>3</sub> under drier conditions. Stem CH<sub>4</sub> fluxes were negatively correlated with the ratio of methanogenesis to methanotrophy genes, highlighting a potential decoupling of stem CH<sub>4</sub> emissions from soil processes.

Annual stem N<sub>2</sub>O fluxes were positively driven by WTD and SWC, while having negative relationships with soil and air temperature (Table 3). Negative correlations also emerged between birch N<sub>2</sub>O fluxes and soil NO<sub>3</sub> content. The short-lived peaks observed in the temporal dynamics of birch stem N<sub>2</sub>O emissions coinciding with increases in SWC (Figure 3A; 3C) agree with previous studies suggesting that stem N<sub>2</sub>O emissions can be induced by rapid changes in soil hydrological conditions, such as freeze-thaw or flooding events or wet and dry period transitions (Mander et al., 2021; Schindler et al., 2020). The inverse relationships with soil and air temperatures emerge due to peak emissions occurring in autumn and spring when temperatures are lower. Therefore, soil water status plays a greater role in driving stem N<sub>2</sub>O fluxes, particularly the emission peaks, than temperature dynamics. Higher-frequency measurements could help capture these emissions' peaks more precisely, enabling more accurate estimation of the total contribution of stem fluxes on the annual forest GHG budgets (Barba

et al., 2019b; Barton et al., 2015). Similar to stem CH<sub>4</sub> flux dynamics, the relationships between stem N<sub>2</sub>O fluxes and environmental factors were reversed in the springtime (Article IV), with fluxes correlating negatively with soil hydrological variables and positively with air temperature and PAR. While WTD and SWC were in a gradual decline during the spring, stem flux variations corresponded to temperature dynamics. If SWC remained in the optimum range for soil N<sub>2</sub>O production, temperature could have taken over as the primary driver of flux variability. Positive relationships between fluxes and PAR could either be due to indirect effects through temperature or showing the influence of plant physiological activity on stem N<sub>2</sub>O fluxes. As a hot moment of N<sub>2</sub>O release was likely not observed during the study period in Article IV, it is possible that outside of the peak periods, stem N<sub>2</sub>O release is more driven by temperature changes, provided that SWC is in optimum range, and the peaks in emissions are induced by rapid changes in soil hydrology.

Tree stem CO<sub>2</sub> efflux followed the trend of the growing season, with fluxes highly dependent on air and soil temperatures, while having negative relationships with hydrological variables (Table 3). Therefore, in contrast to stem CH<sub>4</sub> and N<sub>2</sub>O dynamics, average stem CO<sub>2</sub> release was higher during the drier period (Table 2) with temperature being the primary determinant of the efflux (Table 3). This has also been reported in previous studies (Barba et al., 2019b; Takahashi et al., 2022; Zha, 2004), related to temperature sensitivity of stem respiration processes and diffusion rates (Teskey et al., 2008), as well as reduced transpiration and the resulting higher concentrations of gaseous CO<sub>2</sub> in the stem (Salomón et al., 2016). Furthermore, PAR was also a significant driver of fluxes in the springtime, indicating the influence of photosynthesis and the associated tree growth on respiration (Zha, 2004). Thus, the temporal dynamics of CO<sub>2</sub> fluxes were linked to plant phenological and physiological activity even during the early growing season. Additionally, while SWC and WTD may have affected stem CO<sub>2</sub> fluxes indirectly due to their own dependence on temperature dynamics, the negative relationship with soil hydrological variables can also be attributed to higher stem water content in wetter conditions, which increases resistance to radial diffusion (Bowman et al., 2005; Gansert & Burgdorf, 2005; Salomón et al., 2016).

Furthermore, the relationships between tree stem CH<sub>4</sub>, N<sub>2</sub>O and CO<sub>2</sub> fluxes and sap flow rates in a peatland forest were demonstrated for the first time (Article I). Significant correlations were observed between sap flow rates and birch N<sub>2</sub>O fluxes, as well as birch and spruce CO<sub>2</sub> fluxes during the growing season (Figure 7). Previous studies have shown varying degrees of influence of sap flow rates on stem CO<sub>2</sub> efflux (Bowman et al., 2005; Kunert & Edinger, 2015; Maier & Clinton, 2006). However, in-situ evidence of relationships between sap flow and stem CH<sub>4</sub> and N<sub>2</sub>O fluxes remains limited (Barba et al., 2021; Takahashi et al., 2022). Although xylem sap flow has been shown in a laboratory setting to be responsible for the upward transport of soil-produced CH<sub>4</sub> (Anttila et al., 2023), a relationship between sap flow and stem CH<sub>4</sub> flux did not emerge (Figure 7A). Takahashi et al. (2022) demonstrated that sap flow primarily drives diurnal variations in stem CH<sub>4</sub> emissions, whereas other factors were responsible

for longer term changes in fluxes. Barba et al. (2021) also highlighted the effect of sap flow on both diurnal and seasonal variability of stem fluxes, particularly for CO<sub>2</sub> and CH<sub>4</sub>. Therefore, higher frequency stem flux measurements are necessary to accurately assess the relationship between sap flux rates and stem fluxes on different timescales.

The springtime study (Article IV) provided one of the first attempts to link birch stem CH<sub>4</sub> and CO<sub>2</sub> fluxes to the dissolved gas concentrations in birch sap and soil water. Temporal trends showed that increased dCH<sub>4soil</sub> and dCO<sub>2soil</sub> preceded a peak in stem and soil fluxes, as well as increases in dCH<sub>4sap</sub> and dCO<sub>2sap</sub> (Article IV Figure 2). Birch CH<sub>4</sub> fluxes and dCH<sub>4sap</sub> did not follow the same temporal patterns, with the highest CH<sub>4</sub> fluxes occurring prior to the highest sap concentrations. This lack of relationship could indicate that emissions during the early growing season are unrelated to the transpiration stream. In contrast, CO<sub>2</sub> fluxes had significant correlations with dCO<sub>2sap</sub>, with both increasing simultaneously until the highest average values on 25/04/2023. The interpretation of dCO<sub>2sap</sub> is challenging because in addition to sap ascending in the xylem, stem respiration also produces CO<sub>2</sub> along the stem, which can both diffuse into the atmosphere or further dissolve in the xylem sap (Hölttä & Kolari, 2009; Teskey et al., 2008). dCH<sub>4soil</sub> was around 40 times higher than dCH<sub>4sap</sub>, while dCO<sub>2soil</sub> and dCO<sub>2sap</sub> remained in the same scale. This suggests that some of the CH<sub>4</sub> could be oxidised by methanotrophs in the stem during its ascent in the soil-stem transpiration stream (Putkinen et al., 2021). However, previous studies have reported primarily diurnal variations in CO<sub>2</sub> concentrations in xylem sap (McGuire & Teskey, 2004; Saveyn et al., 2007), while CH<sub>4</sub> remains unstudied. Water ascent from tree roots through the xylem can occur within hours, potentially revealing shorter-term time lags between soil and stem dissolved gas concentrations and fluxes (Schenk et al., 2016). Thus, investigating diurnal variations in stem fluxes, along with sap flow rates and dissolved gas concentrations, could enhance our understanding of plant hydraulics and its effect on fluxes. Isotopic studies could further determine the depth of root water uptake. While recent efforts have aimed to elucidate the specific effects of plant hydraulics (Megonigal et al., 2020) and tree stem physiological traits (Jeffrey et al., 2023a) on stem GHG fluxes, this research avenue remains relatively understudied.

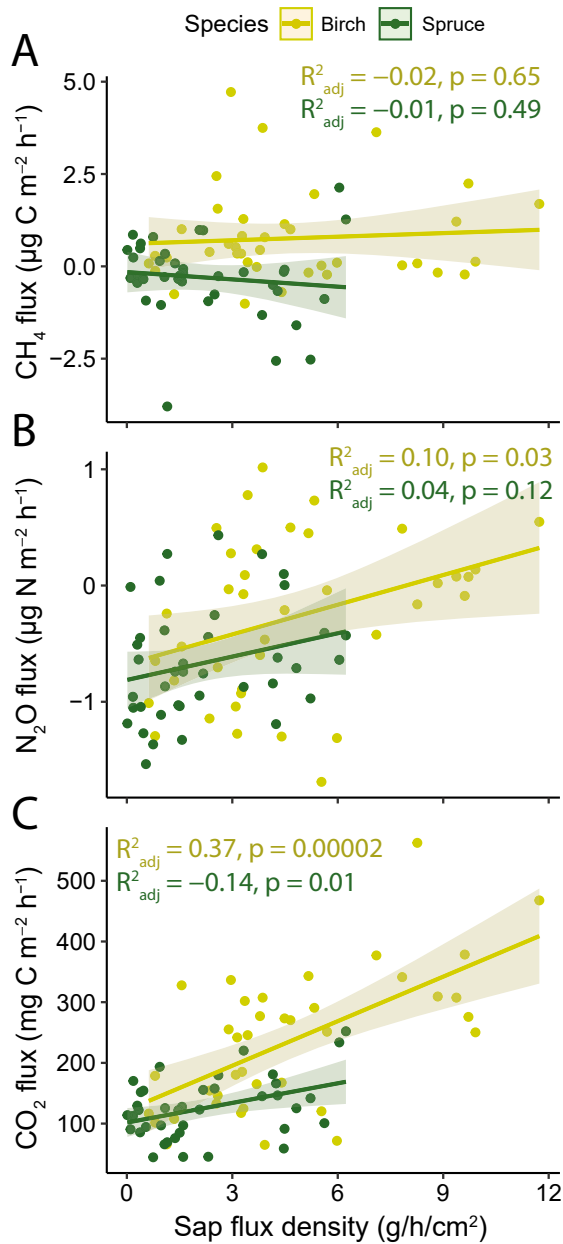


Figure 7. Relationship between sap flow density and birch (n=39) and spruce (n=39) stem (A)  $\text{CH}_4$ , (B)  $\text{N}_2\text{O}$  and (C)  $\text{CO}_2$  fluxes during the growing season (04 June 2021–06 September 2021). Adjusted  $R^2$  and  $p$ -values of the relationships have been calculated according to the linear regression model. Modified from Article I with the 95% confidence interval added as shaded areas.

### 2.2.3. Origin of stem fluxes

Dissecting the origin of stem-emitted gases remains a challenge in stem flux studies (Barba et al., 2019a; Jeffrey et al., 2021; Pitz & Megonigal, 2017). The vertical stem flux profile, together with relationships between stem fluxes and soil environmental parameters, can give insights into the origin of the released gases. The results suggested that the net stem CH<sub>4</sub> flux may have been an aggregate of soil derived CH<sub>4</sub> and CH<sub>4</sub> produced microbially inside or on the tree stem. No statistically significant vertical patterns were observed for stem CH<sub>4</sub> fluxes for either species (Figure 8A), and xylem sap flow was not driving CH<sub>4</sub> fluxes during the growing season (Figure 7A). However, stem CH<sub>4</sub> fluxes were significantly related to soil environmental variables (Table 3). As the soil constituted a net CH<sub>4</sub> sink while stems remained a source, the soil-derived CH<sub>4</sub> must have originated from deeper soil layers, where anaerobic conditions and methanogenesis prevail (Machacova et al., 2023; Pitz et al., 2018). For N<sub>2</sub>O, birch stem fluxes decreased with increasing stem height (Figure 8B) and were related to sap flow rates (Figure 7B), indicating a dominant soil source for birch stem N<sub>2</sub>O fluxes, supported by their correlation with soil N<sub>2</sub>O emissions and environmental variables (Table 3). In contrast, spruce N<sub>2</sub>O fluxes were negligible with minor uptake, which has been explained in the previous chapters. Stem-emitted CO<sub>2</sub> primarily results from a combination of root respiration, stem respiration, and, to a lesser extent, root-uptake of CO<sub>2</sub> dissolved in soil water (Aubrey & Teskey, 2009; Bloemen et al., 2013). The results suggested that birch and spruce CO<sub>2</sub> fluxes were driven more by root respiration and root-uptake of CO<sub>2</sub>. This was evidenced by higher fluxes from the lowest part of the stem (Figure 8C), as well as significant relationships with soil CO<sub>2</sub> fluxes (Table 3) and xylem sap flow (Figure 7C). Previous studies have shown varied vertical stem CO<sub>2</sub> flux gradients, as CO<sub>2</sub> produced by stem respiration can dissolve and be transported away from the production location (Salomón et al., 2024). Sap flow rates and CO<sub>2</sub> efflux from stems are both highly dependent on air temperature (Hölttä & Kolari, 2009), and thus, relationships between the two should be further investigated independently of the temperature effect.

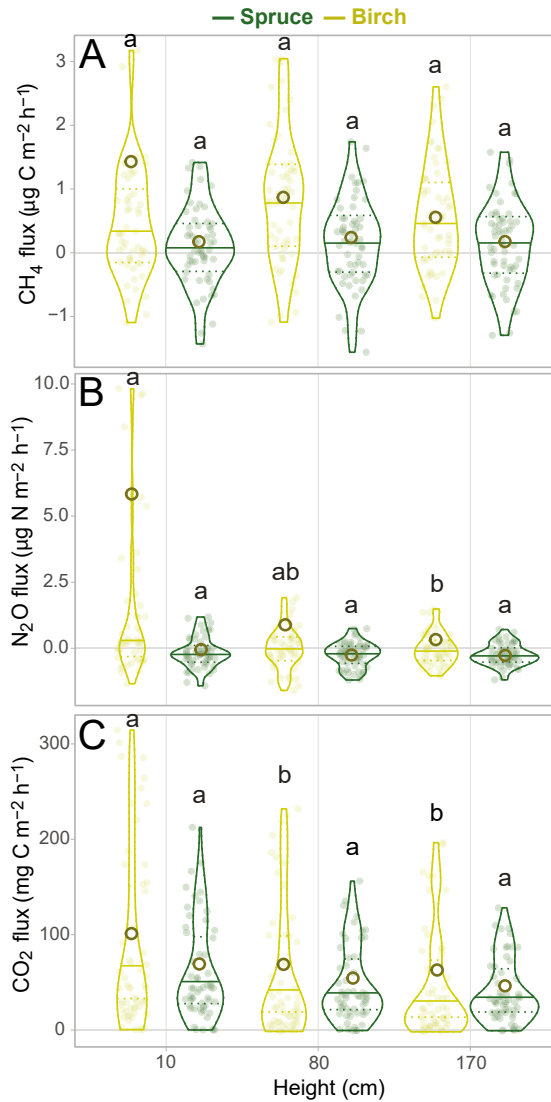


Figure 8. Vertical profile of (A)  $\text{CH}_4$ , (B)  $\text{N}_2\text{O}$  and (C)  $\text{CO}_2$  stem fluxes at 0.1 m, 0.8 m and 1.7 m, averaged across all plots and throughout the annual study period. Different letters above bars indicate statistically significant differences between fluxes at different heights within species, according to a Kruskal-Wallis one-way analysis of variance followed by a post-hoc Dunn test ( $p < 0.05$ ). The solid line within each box marks the median value, circles the mean value and dotted lines the 25th and 75th percentiles. (Article I)

#### 2.2.4. Relative contributions of stem and soil fluxes

Tree stem GHG fluxes can substantially contribute to the combined soil and stem fluxes and neglecting them from forest GHG inventories can lead to under- or overestimation of the gas budgets (Machacova et al., 2023). On an annual scale, birch and spruce stem CH<sub>4</sub> emissions offset the soil sink by 25.9% and 1.9%, respectively (Figure 9A). The potential of trees to offset the soil CH<sub>4</sub> sink has primarily been observed in temperate upland forests (Machacova et al., 2023; Pitz & Magonigal, 2017; Wang et al., 2016). In wetter ecosystems where soil is a net CH<sub>4</sub> source, stem fluxes can add up to 83% to the total soil source in different wetland forests (Jeffrey et al., 2023a; Mander et al., 2022; Pangala et al., 2015). The contribution of stems to total annual N<sub>2</sub>O emissions remained relatively low, adding 3.0% to the soil N<sub>2</sub>O source, almost entirely from birch emissions (Figure 9B). Similar low contributions have been reported in a boreal forest (birch 0.75% and spruce 2.5%) (Machacova et al., 2019), and a riparian forest (alder 0.8%) (Mander et al., 2021). Stem fluxes accounted for 81% of the total CO<sub>2</sub> release during the measurement period (birch 52.4% and spruce 28.6%) (Figure 9C). Although long-term stem CO<sub>2</sub> flux monitoring is rare, growing season stem flux contributions of 28.4% have been shown in a temperate upland forest (Warner et al., 2017).

The findings in Article I indicated significant differences in stem flux contributions between wetter and drier periods, with the differences varying depending on the respective gas (Figure 9). During the drier period, stem CH<sub>4</sub> emissions were negligible while the soil became a major CH<sub>4</sub> sink. In contrast, during the wetter period, soil CH<sub>4</sub> uptake decreased while stem emissions increased, offsetting the soil sink by 40.6% in total (Figure 9A). Previous studies have shown the potential of stem emissions to turn a riparian forest from a sink to a source during the wet period (Mander et al., 2022). These findings further emphasise the strong effect of soil hydrological conditions on stem and soil CH<sub>4</sub> dynamics and the associated CH<sub>4</sub> budget. On the other hand, stem N<sub>2</sub>O flux contributions remained low regardless of wet or dry periods (Figure 9B). The small variation highlights that stem N<sub>2</sub>O fluxes can better respond to short-term hydrological changes, such as freeze-thaw events, flooding, and drought (Mander et al., 2021; Schindler et al., 2020), rather than seasonal wet and dry period variations. Total CO<sub>2</sub> efflux was higher during the drier period, whereas the relative contribution of stem fluxes was more prevalent during the wetter period (Figure 9C). This further emphasises temperature as a primary driver of soil and stem CO<sub>2</sub> dynamics, while hydrological conditions have a secondary effect (Etzold et al., 2013; Kolari et al., 2009). It is crucial to highlight that upscaling chamber measurements, typically conducted at the bottom parts of the stems, to tree-level fluxes is one of the key uncertainties in stem flux studies (Barba et al., 2024), potentially leading to inaccuracies in the contribution of stem fluxes to total ecosystem fluxes.

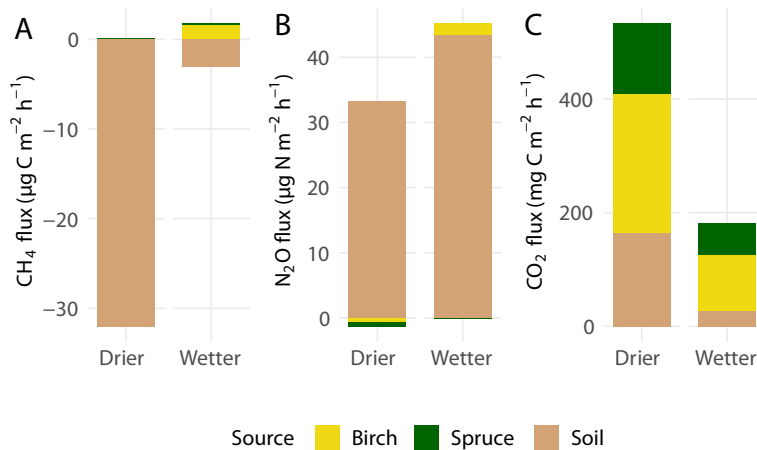


Figure 9. Contributions of average birch, spruce and soil (A) CH<sub>4</sub>, (B) N<sub>2</sub>O and (C) CO<sub>2</sub> fluxes during the drier and wetter periods of the year, scaled to a unit of ground area of forest. The drier period was defined by SWC being continuously < 0.3 m<sup>3</sup>m<sup>-3</sup>. Wetter period: 4 December 2020–12 July 2021; drier period: 13 July 2021–19 August 2021. Note that both stem and soil flux data from these date ranges were used for contributions' calculations as soil flux data was only available between 4 December 2020–19 August 2021. Positive flux values indicate gas emission, negative values uptake. The boxes represent mean fluxes across all measurement points. (Article I)

### 3. CONCLUSIONS

On an annual scale, the soil acted as a net sink of atmospheric CH<sub>4</sub>, and a source of N<sub>2</sub>O and CO<sub>2</sub>. Higher WTD and SWC kept CH<sub>4</sub> fluxes near-zero during the dormant season, switching to significant CH<sub>4</sub> uptake in the drier summer period. Soil hydrology significantly impacted CH<sub>4</sub> dynamics long-term, while temperature was a short-term governing factor. Therefore, hypothesis I was not confirmed, and hypothesis II partially confirmed for soil CH<sub>4</sub> fluxes. Both hypotheses I and II were confirmed for soil N<sub>2</sub>O fluxes, as their temporal dynamics were driven by hot moments of emissions, induced by rapid changes in SWC, such as freeze-thaw events. Soil thawing increased N<sub>2</sub>O emissions, primarily due to incomplete denitrification under prolonged anaerobic conditions, supporting hypothesis III.

Tree stems were net emitters of CH<sub>4</sub>, N<sub>2</sub>O, and CO<sub>2</sub>, with species-specific differences. Birch stems had a greater impact on annual GHG dynamics than spruce stems. Stem CH<sub>4</sub> and N<sub>2</sub>O fluxes exhibited isolated emission peaks, driven by prolonged wetter periods for CH<sub>4</sub> and rapid hydrological changes for N<sub>2</sub>O, supporting hypothesis II. Both soil and stem CO<sub>2</sub> release followed a seasonal pattern, with fluxes highly dependent on temperature. Stem-emitted GHGs likely had a predominantly belowground origin, agreeing with hypothesis IV. Stem CH<sub>4</sub> emissions offset nearly a third of the soil sink annually, rising to almost half during wetter periods, underscoring the significant influence of soil hydrological conditions on CH<sub>4</sub> dynamics. Stem N<sub>2</sub>O fluxes were sensitive to short-term changes in soil hydrology, and their contribution to total N<sub>2</sub>O emissions remained low. CO<sub>2</sub> emitted from the stems constituted a substantial portion of the annual combined soil and stem flux. These findings emphasise that neglecting stem fluxes can result in inaccurate forest GHG budget estimations.

Future research should prioritise several key areas to advance our understanding of tree stem and soil GHG fluxes. Significant uncertainties and knowledge gaps persist in stem flux studies. Further exploration of water movement and dissolved gases in the stem could reveal plant hydraulics' influence on stem fluxes. Isotopic studies could help determine root water uptake depth, clarifying gas transfer pathways. Additionally, microbial analysis of stem core increments could uncover the genetic potential for GHG production or consumption within stems. Long-term, higher-frequency flux measurements from both soil and tree stems could enhance our understanding of flux contributions of different sources to annual forest GHG budgets and help identify the drivers of these fluxes. This study highlighted the importance of focusing on periods of the year with peak soil and stem emissions. Higher-frequency measurements could more accurately capture temporal flux variations.

## REFERENCES

- Ahti, T., Hämet-Ahti, L., and Jalas, J. (1968) Vegetation zones and their sections in northwestern Europe. *Annales Botanici Fennici*, 5(3), 169–211.  
<http://www.jstor.org/stable/23724233>
- Anttila, J., Tikkasalo, O. P., Hölttä, T., Lintunen, A., Vainio, E., Leppä, K., Haikarainen, I., Koivula, H., Ghasemi Falk, H., Kohl, L., Launiainen, S., and Pihlatie, M. (2023) Model of methane transport in tree stems: Case study of sap flow and radial diffusion. *Plant, Cell and Environment*. <https://doi.org/10.1111/pce.14718>
- Aronson, E. L., and Helliker, B. R. (2010) Methane flux in non-wetland soils in response to nitrogen addition: a meta-analysis. *Ecology*, 91(11), 3242–3251.  
<https://doi.org/https://doi.org/10.1890/09-2185.1>
- Aubrey, D. P., and Teskey, R. O. (2009) Root-derived CO<sub>2</sub> efflux via xylem stream rivals soil CO<sub>2</sub> efflux. *New Phytologist*, 184(1), 35–40.  
<https://doi.org/10.1111/j.1469-8137.2009.02971.x>
- Bachofen, C., Tumber-Dávila, S. J., Mackay, D. S., McDowell, N. G., Carminati, A., Klein, T., Stocker, B. D., Mencuccini, M., and Grossiord, C. (2024) Tree water uptake patterns across the globe. *New Phytologist*, 242, 1891–1910.  
<https://doi.org/https://doi.org/10.1111/nph.19762>
- Barba, J., Bradford, M. A., Brewer, P. E., Bruhn, D., Covey, K., Haren, J., J, Mikkelsen, T. N., Pangala, S. R., Pihlatie, M., Poulter, B., Rivas-Ubach, A., Schadt, C. W., Tera-zawa, K., Warner, D. L., Zhang, Z., and Vargas, R. (2019a) Methane emissions from tree stems: a new frontier in the global carbon cycle. *New Phytologist*, 222(1), 18–28.  
<https://doi.org/10.1111/nph.15582>
- Barba, J., Poyatos, R., and Vargas, R. (2019b) Automated measurements of greenhouse gases fluxes from tree stems and soils: magnitudes, patterns and drivers. *Scientific Reports*, 9(1). <https://doi.org/10.1038/s41598-019-39663-8>
- Barba, J., Poyatos, R., Capocci, M., and Vargas, R. (2021) Spatiotemporal variability and origin of CO<sub>2</sub> and CH<sub>4</sub> tree stem fluxes in an upland forest. *Global Change Biology*, 27(19), 4879–4893. <https://doi.org/10.1111/gcb.15783>
- Barba, J., Brewer, P. E., Pangala, S. R., and Machacova, K. (2024) Methane emissions from tree stems – current knowledge and challenges: an introduction to a Virtual Issue. *New Phytologist*, 241(4), 1377–1380. <https://doi.org/10.1111/nph.19512>
- Barrat, H. A., Evans, J., Chadwick, D. R., Clark, I. M., Le Cocq, K., and Cardenas, L. (2021) The impact of drought and rewetting on N<sub>2</sub>O emissions from soil in temperate and Mediterranean climates. *European Journal of Soil Science*, 72(6), 2504–2516.  
<https://doi.org/10.1111/ejss.13015>
- Barton, L., Wolf, B., Rowlings, D., Scheer, C., Kiese, R., Grace, P., Stefanova, K., and Butterbach-Bahl, K. (2015) Sampling frequency affects estimates of annual nitrous oxide fluxes. *Scientific Reports*, 5(1), 15912. <https://doi.org/10.1038/srep15912>
- Bloemen, J., McGuire, M. A., Aubrey, D. P., Teskey, R. O., and Steppe, K. (2013) Transport of root-respired CO<sub>2</sub> via the transpiration stream affects aboveground carbon assimilation and CO<sub>2</sub> efflux in trees. *New Phytologist*, 197(2), 555–565.  
<https://doi.org/10.1111/j.1469-8137.2012.04366.x>
- Bodelier, P. L. E., and Laanbroek, H. J. (2004) Nitrogen as a regulatory factor of methane oxidation in soils and sediments. *FEMS Microbiology Ecology*, 47(3), 265–277.  
[https://doi.org/10.1016/s0168-6496\(03\)00304-0](https://doi.org/10.1016/s0168-6496(03)00304-0)

- Borken, W., Davidson, E. A., Savage, K., Sundquist, E. T., and Steudler, P. (2006) Effect of summer throughfall exclusion, summer drought, and winter snow cover on methane fluxes in a temperate forest soil. *Soil Biology and Biochemistry*, 38(6), 1388–1395. <https://doi.org/https://doi.org/10.1016/j.soilbio.2005.10.011>
- Bowman, W. P., Barbour, M. M., Turnbull, M. H., Tissue, D. T., Whitehead, D., and Griffin, K. L. (2005) Sap flow rates and sapwood density are critical factors in within- and between-tree variation in CO<sub>2</sub> efflux from stems of mature *Dacrydium cupressinum* trees. *New Phytologist*, 167(3), 815–828. <https://doi.org/10.1111/j.1469-8137.2005.01478.x>
- Braker, G., and Conrad, R. (2011) Diversity, structure, and size of N<sub>2</sub>O-producing microbial communities in soils—what matters for their functioning? *Advances in applied microbiology*, 75, 33–70. <https://doi.org/https://doi.org/10.1016/B978-0-12-387046-9.00002-5>
- Butterbach-Bahl, K., Willibald, G., and Papen, H. (2002) Soil core method for direct simultaneous determination of N<sub>2</sub> and N<sub>2</sub>O emissions from forest soils. *Plant and Soil*, 240(1), 105–116. <https://doi.org/10.1023/a:1015870518723>
- Butterbach-Bahl, K., Baggs, E. M., Dannenmann, M., Kiese, R., and Zechmeister-Boltenstern, S. (2013) Nitrous oxide emissions from soils: how well do we understand the processes and their controls? *Philosophical Transactions of the Royal Society B: Biological Sciences*, 368(1621), 20130122. <https://doi.org/10.1098/rstb.2013.0122>
- Covey, K. R., and Magonigal, J. P. (2019) Methane production and emissions in trees and forests. *New Phytologist*, 222(1), 35–51. <https://doi.org/10.1111/nph.15624>
- Espenberg, M., Truu, M., Mander, Ü., Kasak, K., Nõlvak, H., Ligi, T., Oopkaup, K., Maddison, M., and Truu, J. (2018) Differences in microbial community structure and nitrogen cycling in natural and drained tropical peatland soils. *Scientific Reports*, 8(1). <https://doi.org/10.1038/s41598-018-23032-y>
- Etzold, S., Zweifel, R., Ruehr, N. K., Eugster, W., and Buchmann, N. (2013) Long-term stem CO<sub>2</sub> concentration measurements in Norway spruce in relation to biotic and abiotic factors. *New Phytologist*, 197(4), 1173–1184. <https://doi.org/10.1111/nph.12115>
- Frolking, S., Talbot, J., Jones, M. C., Treat, C. C., Kauffman, J. B., Tuittila, E.-S., and Roulet, N. (2011) Peatlands in the Earth's 21st century climate system. *Environmental Reviews*, 19, 371–396. <https://doi.org/10.1139/a11-014>
- Gansert, D., and Burgdorf, M. (2005) Effects of xylem sap flow on carbon dioxide efflux from stems of birch (*Betula pendula* Roth). *Flora – Morphology, Distribution, Functional Ecology of Plants*, 200(5), 444–455. <https://doi.org/https://doi.org/10.1016/j.flora.2004.12.005>
- Gauci, V., Gowing, D. J. G., Hornibrook, E. R. C., Davis, J. M., and Dise, N. B. (2010) Woody stem methane emission in mature wetland alder trees. *Atmospheric Environment*, 44(17), 2157–2160. <https://doi.org/10.1016/j.atmosenv.2010.02.034>
- Graf, D. R. H., Jones, C. M., and Hallin, S. (2014) Intergenomic Comparisons Highlight Modularity of the Denitrification Pathway and Underpin the Importance of Community Structure for N<sub>2</sub>O Emissions. *PLoS ONE*, 9(12), e114118. <https://doi.org/10.1371/journal.pone.0114118>
- Groffman, P. M., Hardy, J. P., Driscoll, C. T., and Fahey, T. J. (2006) Snow depth, soil freezing, and fluxes of carbon dioxide, nitrous oxide and methane in a northern hardwood forest. *Global Change Biology*, 12(9), 1748–1760. <https://doi.org/10.1111/j.1365-2486.2006.01194.x>

- Hanson, R. S., and Hanson, T. E. (1996) Methanotrophic bacteria. *Microbiological Reviews*, 60(2), 439–471. <https://doi.org/10.1128/mr.60.2.439-471.1996>
- Henry, H. A. L. (2008) Climate change and soil freezing dynamics: historical trends and projected changes. *Climatic Change*, 87(3–4), 421–434. <https://doi.org/10.1007/s10584-007-9322-8>
- Hölttä, T., and Kolari, P. (2009) Interpretation of stem CO<sub>2</sub> efflux measurements. *Tree Physiology*, 29(11), 1447–1456. <https://doi.org/10.1093/treephys/tpp073>
- Hu, B.-l., Shen, L.-d., Lian, X., Zhu, Q., Liu, S., Huang, Q., He, Z.-f., Geng, S., Cheng, D.-q., Lou, L.-p., Xu, X.-y., Zheng, P., and He, Y.-f. (2014) Evidence for nitrite-dependent anaerobic methane oxidation as a previously overlooked microbial methane sink in wetlands. *Proceedings of the National Academy of Sciences*, 111(12), 4495–4500. <https://doi.org/10.1073/pnas.1318393111>
- Huang, Y., Ciais, P., Luo, Y., Zhu, D., Wang, Y., Qiu, C., Goll, D. S., Guenet, B., Makowski, D., De Graaf, I., Leifeld, J., Kwon, M. J., Hu, J., and Qu, L. (2021) Tradeoff of CO<sub>2</sub> and CH<sub>4</sub> emissions from global peatlands under water-table drawdown. *Nature Climate Change*, 11(7), 618–622. <https://doi.org/10.1038/s41558-021-01059-w>
- Hugelius, G., Loisel, J., Chadburn, S., Jackson, R. B., Jones, M., MacDonald, G., Marshchak, M., Olefeldt, D., Packalen, M., Siewert, M. B., Treat, C., Turetsky, M., Voigt, C., and Yu, Z. (2020) Large stocks of peatland carbon and nitrogen are vulnerable to permafrost thaw. *Proceedings of the National Academy of Sciences*, 117(34), 20438–20446. <https://doi.org/doi:10.1073/pnas.1916387117>
- IUSS Working Group WRB (2015) *World Reference Base for Soil Resources 2014, Update 2015*. World soil resources reports. 106. In: International soil classification system for naming soils and creating legends for soil maps. Food and agriculture Organization of the United Nations, Rome, Italy.
- Järveoja, J., Nilsson, M. B., Gažovič, M., Crill, P. M., and Peichl, M. (2018) Partitioning of the net CO<sub>2</sub> exchange using an automated chamber system reveals plant phenology as key control of production and respiration fluxes in a boreal peatland. *Global Change Biology*, 24(8), 3436–3451. <https://doi.org/10.1111/gcb.14292>
- Jeffrey, L. C., Maher, D. T., Tait, D. R., Euler, S., and Johnston, S. G. (2020) Tree stem methane emissions from subtropical lowland forest (*Melaleuca quinquenervia*) regulated by local and seasonal hydrology. *Biogeochemistry*, 151(2–3), 273–290. <https://doi.org/10.1007/s10533-020-00726-y>
- Jeffrey, L. C., Maher, D. T., Chiri, E., Leung, P. M., Nauer, P. A., Arndt, S. K., Tait, D. R., Greening, C., and Johnston, S. G. (2021) Bark-dwelling methanotrophic bacteria decrease methane emissions from trees. *Nature Communications*, 12(1). <https://doi.org/10.1038/s41467-021-22333-7>
- Jeffrey, L. C., Johnston, S. G., Tait, D. R., Dittmann, J., and Maher, D. T. (2023a) Rapid bark-mediated tree stem methane transport occurs independently of the transpiration stream in *Melaleuca quinquenervia*. *New Phytologist*, 242, 49–60. <https://doi.org/10.1111/nph.19404>
- Jeffrey, L. C., Moras, C. A., Tait, D. R., Johnston, S. G., Call, M., Sippo, J. Z., Jeffrey, N. C., Laicher-Edwards, D., and Maher, D. T. (2023b) Large Methane Emissions From Tree Stems Complicate the Wetland Methane Budget. *Journal of Geophysical Research: Biogeosciences*, 128(12). <https://doi.org/10.1029/2023jg007679>
- Jiang, M., Medlyn, B. E., Drake, J. E., Duursma, R. A., Anderson, I. C., Barton, C. V. M., Boer, M. M., Carrillo, Y., Castañeda-Gómez, L., Collins, L., Crous, K. Y., De Kauwe, M. G., Dos Santos, B. M., Emmerson, K. M., Facey, S. L., Gherlenda, A. N., Gimeno, T. E., Hasegawa, S., Johnson, S. N., Ellsworth, D. S. (2020) The fate of carbon in a

- mature forest under carbon dioxide enrichment. *Nature*, 580(7802), 227–231. <https://doi.org/10.1038/s41586-020-2128-9>
- Kepler, F., Hamilton, J. T. G., Braß, M., and Röckmann, T. (2006) Methane emissions from terrestrial plants under aerobic conditions. *Nature*, 439(7073), 187–191. <https://doi.org/10.1038/nature04420>
- Kim, D. G., Vargas, R., Bond-Lamberty, B., and Turetsky, M. R. (2012) Effects of soil rewetting and thawing on soil gas fluxes: a review of current literature and suggestions for future research. *Biogeosciences*, 9(7), 2459–2483. <https://doi.org/10.5194/bg-9-2459-2012>
- Kolari, P., Kulmala, L., Pumpanen, J., Launiainen, S., Ilvesniemi, H., Hari, P., and Nikinmaa, E. (2009) CO<sub>2</sub> exchange and component CO<sub>2</sub> fluxes of a boreal Scots pine forest. *Boreal Environment Research*, 14(4), 761–783.
- Köppen, W. (1936) Das geographische System der Klimate. 1–44.
- Korkiakoski, M., Tuovinen, J.-P., Aurela, M., Koskinen, M., Minkkinen, K., Ojanen, P., Penttilä, T., Rainne, J., Laurila, T., and Lohila, A. (2017) Methane exchange at the peatland forest floor – automatic chamber system exposes the dynamics of small fluxes. *Biogeosciences*, 14(7), 1947–1967. <https://doi.org/10.5194/bg-14-1947-2017>
- Korkiakoski, M., Tuovinen, J.-P., Penttilä, T., Sarkkola, S., Ojanen, P., Minkkinen, K., Rainne, J., Laurila, T., and Lohila, A. (2019) Greenhouse gas and energy fluxes in a boreal peatland forest after clear-cutting. *Biogeosciences*, 16(19), 3703–3723. <https://doi.org/10.5194/bg-16-3703-2019>
- Kozlowski, T. T. (1997) Responses of woody plants to flooding and salinity. *Tree Physiology*, 17(7), 490–490. <https://doi.org/10.1093/treephys/17.7.490>
- Kunert, N., and Edinger, J. (2015) Xylem Sap Flux Affects Conventional Stem CO<sub>2</sub> Efflux Measurements in Tropical Trees. *Biotropica*, 47(6), 650–653. <https://doi.org/10.1111/btp.12257>
- Kupper, P., Söber, J., Sellin, A., Löhmus, K., Tullus, A., Räm, O., Lubenets, K., Tulva, I., Uri, V., Zobel, M., Kull, O., and Söber, A. (2011) An experimental facility for free air humidity manipulation (FAHM) can alter water flux through deciduous tree canopy. *Environmental and Experimental Botany*, 72(3), 432–438. <https://doi.org/https://doi.org/10.1016/j.envexpbot.2010.09.003>
- Kuypers, M. M. M., Marchant, H. K., and Kartal, B. (2018) The microbial nitrogen-cycling network. *Nature Reviews Microbiology*, 16(5), 263–276. <https://doi.org/10.1038/nrmicro.2018.9>
- Lenhart, K., Weber, B., Elbert, W., Steinkamp, J., Clough, T., Crutzen, P., Pöschl, U., and Kepler, F. (2015) Nitrous oxide and methane emissions from cryptogamic covers. *Global Change Biology*, 21(10), 3889–3900. <https://doi.org/10.1111/gcb.12995>
- Limpens, J., Heijmans, M. M. P. D., and Berendse, F. (2006) The Nitrogen Cycle in Boreal Peatlands. In: Wieder, R.K., Vitt, D.H. (eds) *Boreal Peatland Ecosystems*. pp. 195–230. Springer, Berlin Heidelberg. [https://doi.org/10.1007/978-3-540-31913-9\\_10](https://doi.org/10.1007/978-3-540-31913-9_10)
- Lohila, A., Minkkinen, K., Aurela, M., Tuovinen, J. P., Penttilä, T., Ojanen, P., and Laurila, T. (2011) Greenhouse gas flux measurements in a forestry-drained peatland indicate a large carbon sink. *Biogeosciences*, 8(11), 3203–3218. <https://doi.org/10.5194/bg-8-3203-2011>
- Löhmus, E. (1984) *Eesti metsakasvukohatüübid*.

- Ma, W. K., Schautz, A., Fishback, L.-A. E., Bedard-Haughn, A., Farrell, R. E., and Sicialiano, S. D. (2007) Assessing the potential of ammonia oxidizing bacteria to produce nitrous oxide in soils of a high arctic lowland ecosystem on Devon Island, Canada. *Soil Biology and Biochemistry*, 39(8), 2001–2013. <https://doi.org/https://doi.org/10.1016/j.soilbio.2007.03.001>
- Machacova, K., Bäck, J., Vanhatalo, A., Halmeenmäki, E., Kolari, P., Mammarella, I., Pumpanen, J., Acosta, M., Urban, O., and Pihlatie, M. (2016) *Pinus sylvestris* as a missing source of nitrous oxide and methane in boreal forest. *Scientific Reports*, 6(1), 23410. <https://doi.org/10.1038/srep23410>
- Machacova, K., Maier, M., Svobodova, K., Lang, F., and Urban, O. (2017) Cryptogamic stem covers may contribute to nitrous oxide consumption by mature beech trees. *Scientific Reports*, 7(1) <https://doi.org/10.1038/s41598-017-13781-7>
- Machacova, K., Vainio, E., Urban, O., and Pihlatie, M. (2019) Seasonal dynamics of stem N<sub>2</sub>O exchange follow the physiological activity of boreal trees. *Nature Communications*, 10(1) <https://doi.org/10.1038/s41467-019-12976-y>
- Machacova, K., Warlo, H., Svobodová, K., Agyei, T., Uchytlová, T., Horáček, P., and Lang, F. (2023) Methane emission from stems of European beech (*Fagus sylvatica*) offsets as much as half of methane oxidation in soil. *New Phytologist*, 238(2), 584–597. <https://doi.org/10.1111/nph.18726>
- Magen, C., Lapham, L. L., Pohlman, J. W., Marshall, K., Bosman, S., Casso, M., and Chanton, J. P. (2014) A simple headspace equilibration method for measuring dissolved methane. *Limnology and Oceanography: Methods*, 12(9), 637–650. <https://doi.org/10.4319/lom.2014.12.637>
- Maier, C. A., and Clinton, B. D. (2006) Relationship between stem CO<sub>2</sub> efflux, stem sap velocity and xylem CO<sub>2</sub> concentration in young loblolly pine trees. *Plant, Cell and Environment*, 29(8), 1471–1483. <https://doi.org/10.1111/j.1365-3040.2006.01511.x>
- Maljanen, M., Hytönen, J., and Martikainen, P. J. (2010) Cold-season nitrous oxide dynamics in a drained boreal peatland differ depending on land-use practice. *Canadian Journal of Forest Research*, 40(3), 565–572. <https://doi.org/10.1139/X10-004>
- Mander, Ü., Krasnova, A., Escuer-Gatius, J., Espenberg, M., Schindler, T., Machacova, K., Pärn, J., Maddison, M., Megonigal, J. P., Pihlatie, M., Kasak, K., Niinemets, Ü., Junninen, H., and Soosaar, K. (2021) Forest canopy mitigates soil N<sub>2</sub>O emission during hot moments. *Npj Climate and Atmospheric Science*, 4(1) <https://doi.org/10.1038/s41612-021-00194-7>
- Mander, Ü., Krasnova, A., Schindler, T., Megonigal, J. P., Escuer-Gatius, J., Espenberg, M., Machacova, K., Maddison, M., Pärn, J., Ranniku, R., Pihlatie, M., Kasak, K., Niinemets, Ü., and Soosaar, K. (2022) Long-term dynamics of soil, tree stem and ecosystem methane fluxes in a riparian forest. *Science of The Total Environment*, 809, 151723. <https://doi.org/https://doi.org/10.1016/j.scitotenv.2021.151723>
- McGuire, M. A., and Teskey, R. O. (2004) Estimating stem respiration in trees by a mass balance approach that accounts for internal and external fluxes of CO<sub>2</sub>. *Tree Physiology*, 24(5), 571–578. <https://doi.org/10.1093/treephys/24.5.571>
- Megonigal, J. P., Brewer, P. E., and Knee, K. L. (2020) Radon as a natural tracer of gas transport through trees. *New Phytologist*, 225(4), 1470–1475. <https://doi.org/10.1111/nph.16292>
- Minkinen, K., Laine, J., Shurpali, N. J., Maekiranta, P., Alm, J., and Penttilä, T. (2007) Heterotrophic soil respiration in forestry-drained peatlands. *Boreal Environment Research*, 12(2), 115–126.

- Moldaschl, E., Kitzler, B., Machacova, K., Schindler, T., and Schindlbacher, A. (2021) Stem CH<sub>4</sub> and N<sub>2</sub>O fluxes of *Fraxinus excelsior* and *Populus alba* trees along a flooding gradient. *Plant and Soil*, 461(1–2), 407–420. <https://doi.org/10.1007/s11104-020-04818-4>
- Ni, X., and Groffman, P. M. (2018) Declines in methane uptake in forest soils. *Proceedings of the National Academy of Sciences*, 115(34), 8587–8590. <https://doi.org/10.1073/pnas.1807377115>
- Ojanen, P., Minkkinen, K., Alm, J., and Penttilä, T. (2010) Soil–atmosphere CO<sub>2</sub>, CH<sub>4</sub> and N<sub>2</sub>O fluxes in boreal forestry-drained peatlands. *Forest Ecology and Management*, 260(3), 411–421. <https://doi.org/10.1016/j.foreco.2010.04.036>
- Öquist, M. G., Nilsson, M., Sörensson, F., Kasimir-Klemedtsson, Å., Persson, T., Weslien, P., and Klemedtsson, L. (2004) Nitrous oxide production in a forest soil at low temperatures – processes and environmental controls. *FEMS Microbiology Ecology*, 49(3), 371–378. <https://doi.org/10.1016/j.femsec.2004.04.006>
- Pangala, S. R., Hornibrook, E. R. C., Gowing, D. J., and Gauci, V. (2015) The contribution of trees to ecosystem methane emissions in a temperate forested wetland. *Global Change Biology*, 21(7), 2642–2654. <https://doi.org/10.1111/gcb.12891>
- Pangala, S. R., Moore, S., Hornibrook, E. R. C., and Gauci, V. (2013) Trees are major conduits for methane egress from tropical forested wetlands. *New Phytologist*, 197(2), 524–531. <https://doi.org/10.1111/nph.12031>
- Pett-Ridge, J., Petersen, D. G., Nuccio, E., and Firestone, M. K. (2013) Influence of oxic/anoxic fluctuations on ammonia oxidizers and nitrification potential in a wet tropical soil. *FEMS Microbiology Ecology*, 85(1), 179–194. <https://doi.org/10.1111/1574-6941.12111>
- Pihlatie, M. K., Kiese, R., Brüggemann, N., Butterbach-Bahl, K., Kieloaho, A. J., Laurila, T., Lohila, A., Mammarella, I., Minkkinen, K., Penttilä, T., Schönborn, J., and Vesala, T. (2010) Greenhouse gas fluxes in a drained peatland forest during spring frost-thaw event. *Biogeosciences*, 7(5), 1715–1727. <https://doi.org/10.5194/bg-7-1715-2010>
- Pitz, S., and Megonigal, J. P. (2017) Temperate forest methane sink diminished by tree emissions. *New Phytologist*, 214(4), 1432–1439. <https://doi.org/10.1111/nph.14559>
- Pitz, S. L., Megonigal, J. P., Chang, C.-H., and Szlavecz, K. (2018) Methane fluxes from tree stems and soils along a habitat gradient. *Biogeochemistry*, 137(3), 307–320. <https://doi.org/10.1007/s10533-017-0400-3>
- Puhe, J. (2003) Growth and development of the root system of Norway spruce (*Picea abies*) in forest stands—a review. *Forest Ecology and Management*, 175(1), 253–273. [https://doi.org/https://doi.org/10.1016/S0378-1127\(02\)00134-2](https://doi.org/https://doi.org/10.1016/S0378-1127(02)00134-2)
- Putkinen, A., Siljanen, H. M. P., Laihonon, A., Paasisalo, I., Porkka, K., Tirola, M., Haikarainen, I., Tenhoviirta, S., and Pihlatie, M. (2021) New insight to the role of microbes in the methane exchange in trees: evidence from metagenomic sequencing. *New Phytologist*, 231(2), 524–536. <https://doi.org/10.1111/nph.17365>
- R core team. (2020) R: A language and environment for statistical computing. In Vienna, Austria: R Foundation for Statistical Computing.
- Salomón, R. L., Valbuena-Carabaña, M., Gil, L., McGuire, M. A., Teskey, R. O., Aubrey, D. P., González-Doncel, I., and Rodríguez-Calcerrada, J. (2016) Temporal and spatial patterns of internal and external stem CO<sub>2</sub> fluxes in a sub-Mediterranean oak. *Tree Physiology*, 36(11), 1409–1421. <https://doi.org/10.1093/treephys/tpw029>

- Salomón, R. L., De Roo, L., Bodé, S., Boeckx, P., and Steppe, K. (2021) Efflux and assimilation of xylem-transported CO<sub>2</sub> in stems and leaves of tree species with different wood anatomy. *Plant, Cell and Environment*, *44*(11), 3494–3508. <https://doi.org/10.1111/pce.14062>
- Salomón, R. L., Helm, J., Gessler, A., Grams, T. E. E., Hilman, B., Muhr, J., Steppe, K., Wittmann, C., and Hartmann, H. (2024) The quandary of sources and sinks of CO<sub>2</sub> efflux in tree stems—new insights and future directions. *Tree Physiology*, *44*(1), tpad157. <https://doi.org/10.1093/treephys/tpad157>
- Saveyn, A., Steppe, K., and Lemeur, R. (2007) Drought and the diurnal patterns of stem CO<sub>2</sub> efflux and xylem CO<sub>2</sub> concentration in young oak (*Quercus robur*) *Tree Physiology*, *27*(3), 365–374. <https://doi.org/10.1093/treephys/27.3.365>
- Schenk, H. J., Espino, S., Visser, A., and Esser, B. K. (2016) Dissolved atmospheric gas in xylem sap measured with membrane inlet mass spectrometry. *Plant, Cell and Environment*, *39*(4), 944–950. <https://doi.org/10.1111/pce.12678>
- Schindlbacher, A., Zechmeister-Boltenstern, S., and Jandl, R. (2009) Carbon losses due to soil warming: Do autotrophic and heterotrophic soil respiration respond equally? *Global Change Biology*, *15*(4), 901–913. <https://doi.org/10.1111/j.1365-2486.2008.01757.x>
- Schindler, T., Mander, Ü., Machacova, K., Espenberg, M., Krasnov, D., Escuer-Gatius, J., Veber, G., Pärn, J., and Soosaar, K. (2020) Short-term flooding increases CH<sub>4</sub> and N<sub>2</sub>O emissions from trees in a riparian forest soil-stem continuum. *Scientific Reports*, *10*(1) <https://doi.org/10.1038/s41598-020-60058-7>
- Sjögersten, S., Siegenthaler, A., Lopez, O. R., Aplin, P., Turner, B., and Gauci, V. (2020) Methane emissions from tree stems in neotropical peatlands. *New Phytologist*, *225*(2), 769–781. <https://doi.org/10.1111/nph.16178>
- Smith, J., Wagner-Riddle, C., and Dunfield, K. (2010) Season and management related changes in the diversity of nitrifying and denitrifying bacteria over winter and spring. *Applied Soil Ecology*, *44*(2), 138–146. <https://doi.org/https://doi.org/10.1016/j.apsoil.2009.11.004>
- Takahashi, K., Sakabe, A., Azuma, W. A., Itoh, M., Imai, T., Matsumura, Y., Tateishi, M., and Kosugi, Y. (2022) Insights into the mechanism of diurnal variations in methane emission from the stem surfaces of *Alnus japonica*. *New Phytologist*, *235*(5), 1757–1766. <https://doi.org/10.1111/nph.18283>
- Teepe, R., Brumme, R., and Beese, F. (2001) Nitrous oxide emissions from soil during freezing and thawing periods. *Soil Biology and Biochemistry*, *33*(9), 1269–1275. [https://doi.org/https://doi.org/10.1016/S0038-0717\(01\)00084-0](https://doi.org/https://doi.org/10.1016/S0038-0717(01)00084-0)
- Teepe, R., Vor, A., Beese, F., and Ludwig, B. (2004) Emissions of N<sub>2</sub>O from soils during cycles of freezing and thawing and the effects of soil water, texture and duration of freezing. *European Journal of Soil Science*, *55*(2), 357–365. <https://doi.org/10.1111/j.1365-2389.2004.00602.x>
- Terazawa, K., Yamada, K., Ohno, Y., Sakata, T., and Ishizuka, S. (2015) Spatial and temporal variability in methane emissions from tree stems of *Fraxinus mandshurica* in a cool-temperate floodplain forest. *Biogeochemistry*, *123*(3), 349–362. <https://doi.org/10.1007/s10533-015-0070-y>
- Teskey, R. O., Saveyn, A., Steppe, K., and McGuire, M. A. (2008) Origin, fate and significance of CO<sub>2</sub> in tree stems. *New Phytologist*, *177*(1), 17–32. <https://doi.org/10.1111/j.1469-8137.2007.02286.x>

- Ueda, M. U., Tokuchi, N., and Hiura, T. (2015) Soil nitrogen pools and plant uptake at sub-zero soil temperature in a cool temperate forest soil: a field experiment using  $^{15}\text{N}$  labeling. *Plant and Soil*, 392(1–2), 205–214.  
<https://doi.org/10.1007/s11104-015-2453-1>
- Uri, V., Kukumägi, M., Aosaar, J., Varik, M., Becker, H., Morozov, G., & Karoles, K. (2017) Ecosystems carbon budgets of differently aged downy birch stands growing on well-drained peatlands. *Forest Ecology and Management*, 399, 82–93.  
<https://doi.org/https://doi.org/10.1016/j.foreco.2017.05.023>
- Vainio, E., Haikarainen, I. P., Machacova, K., Putkinen, A., Santalahti, M., Koskinen, M., Fritze, H., Tuomivirta, T., and Pihlatie, M. (2022) Soil-tree-atmosphere  $\text{CH}_4$  flux dynamics of boreal birch and spruce trees during spring leaf-out. *Plant and Soil*, 478(1–2), 391–407. <https://doi.org/10.1007/s11104-022-05447-9>
- Veldkamp, E., Koehler, B., and Corre, M. D. (2013) Indications of nitrogen-limited methane uptake in tropical forest soils. *Biogeosciences*, 10(8), 5367–5379.  
<https://doi.org/10.5194/bg-10-5367-2013>
- Wagner-Riddle, C., Hu, Q. C., Van Bochove, E., and Jayasundara, S. (2008) Linking Nitrous Oxide Flux During Spring Thaw to Nitrate Denitrification in the Soil Profile. *Soil Science Society of America Journal*, 72(4), 908–916.  
<https://doi.org/10.2136/sssaj2007.0353>
- Wagner-Riddle, C., Rapai, J., Warland, J., and Furon, A. (2010) Nitrous oxide fluxes related to soil freeze and thaw periods identified using heat pulse probes. *Canadian Journal of Soil Science*, 90(3), 409–418. <https://doi.org/10.4141/CJSS09016>
- Wang, L., Xu, H., Liu, C., Yang, M., Zhong, J., Wang, W., Li, Z., and Li, K. (2022) Stronger link of *nosZI* than *nosZII* to the higher total  $\text{N}_2\text{O}$  consumption in anoxic paddy surface soils. *Geoderma*, 425, 116035.  
<https://doi.org/https://doi.org/10.1016/j.geoderma.2022.116035>
- Wang, X., Mao, Z., McGuire, M. A., and Teskey, R. O. (2019) Stem radial  $\text{CO}_2$  conductance affects stem respiratory  $\text{CO}_2$  fluxes in ash and birch trees. *Journal of Forestry Research*, 30(1), 21–29. <https://doi.org/10.1007/s11676-018-0737-z>
- Wang, X., Wang, S., Yang, Y., Tian, H., Jetten, M. S. M., Song, C., and Zhu, G. (2023) Hot moment of  $\text{N}_2\text{O}$  emissions in seasonally frozen peatlands. *The ISME Journal*. <https://doi.org/10.1038/s41396-023-01389-x>
- Wang, Z. P., Gu, Q., Deng, F. D., Huang, J. H., Megonigal, J. P., Yu, Q., Lü, X. T., Li, L. H., Chang, S., Zhang, Y. H., Feng, J. C., and Han, X. G. (2016) Methane emissions from the trunks of living trees on upland soils. *New Phytologist*, 211(2), 429–439.  
<https://doi.org/10.1111/nph.13909>
- Warner, D. L., Villarreal, S., McWilliams, K., Inamdar, S., and Vargas, R. (2017) Carbon Dioxide and Methane Fluxes From Tree Stems, Coarse Woody Debris, and Soils in an Upland Temperate Forest. *Ecosystems*, 20(6), 1205–1216.  
<https://doi.org/10.1007/s10021-016-0106-8>
- Wen, Y., Corre, M. D., Rachow, C., Chen, L., and Veldkamp, E. (2017) Nitrous oxide emissions from stems of alder, beech and spruce in a temperate forest. *Plant and Soil*, 420(1–2), 423–434. <https://doi.org/10.1007/s11104-017-3416-5>
- Wu, H., Xingkai, X., Cheng, W., and Lin, H. (2020) Dissolved organic matter and inorganic N jointly regulate greenhouse gases fluxes from forest soils with different moistures during a freeze-thaw period. *Soil Science and Plant Nutrition*, 66(1), 163–176. <https://doi.org/10.1080/00380768.2019.1667212>

- Xu, J., Morris, P. J., Liu, J., and Holden, J. (2018) PEATMAP: Refining estimates of global peatland distribution based on a meta-analysis. *CATENA*, 160, 134–140. <https://doi.org/10.1016/j.catena.2017.09.010>
- Yip, D. Z., Veach, A. M., Yang, Z. K., Cregger, M. A., and Schadt, C. W. (2019) Methanogenic Archaea dominate mature heartwood habitats of Eastern Cottonwood (*Populus deltoides*) *New Phytologist*, 222(1), 115–121. <https://doi.org/10.1111/nph.15346>
- Zha, T. (2004) Seasonal and Annual Stem Respiration of Scots Pine Trees under Boreal Conditions. *Annals of Botany*, 94(6), 889–896. <https://doi.org/10.1093/aob/mch218>
- Zhang, L., Chen, Y., Hao, G., Ma, K., Bongers, F., and Sterck, F. J. (2020) Conifer and broadleaved trees differ in branch allometry but maintain similar functional balances. *Tree Physiology*, 40(4), 511–519. <https://doi.org/10.1093/treephys/tpz139>
- Zhou, L., Wang, Y., Long, X.-E., Guo, J., and Zhu, G. (2014) High abundance and diversity of nitrite-dependent anaerobic methane-oxidizing bacteria in a paddy field profile. *FEMS Microbiology Letters*, 360(1), 33–41. <https://doi.org/10.1111/1574-6968.12567>

## SUMMARY

Peatlands harbour substantial carbon (C) and nitrogen (N) reserves and play a pivotal role in regulating key greenhouse gases (GHGs) such as carbon dioxide (CO<sub>2</sub>), methane (CH<sub>4</sub>), and nitrous oxide (N<sub>2</sub>O), thus impacting global climate. Northern peatlands are often drained to enhance forest productivity. Drainage alters peat soil hydrology, a critical factor governing the balances of GHGs. Lowering the water table can transform these soils from CO<sub>2</sub> sinks to sources, reduce CH<sub>4</sub> emissions, and increase N<sub>2</sub>O release. In addition to soil, tree stems play a crucial role in the GHG budgets of forestry-drained peatlands, though their dynamics are complex and understudied. Simultaneous year-long measurements of soil and tree stem GHG fluxes in northern peatland forests are rare, with previous studies primarily focusing on the growing season and neglecting seasonal variations like spring freeze-thaw cycles.

Accordingly, the objective of this doctoral thesis was to characterise the seasonal variations and key environmental drivers of tree stem and soil CH<sub>4</sub>, N<sub>2</sub>O and CO<sub>2</sub> fluxes in a northern drained peatland forest. Furthermore, the study aimed to explore the impact of soil chemistry and microbial communities on GHG emissions and shed light on the origin of stem fluxes. To achieve this, tree stem and soil GHG fluxes were measured concurrently over a year in a hemiboreal drained peatland forest (Article I), with more specific focus on the previously understudied winter period (Article II). As the importance of spring freeze-thaw periods was emphasised in Articles I and II, a soil warming experiment was conducted (Article III) to investigate N<sub>2</sub>O emission processes and soil microbial abundances during freeze-thaw cycles. Additionally, springtime stem and soil fluxes were studied alongside dissolved gases in birch sap, and the underlying soil microbiome (Article IV).

The study was conducted in a drained peatland forest site in eastern Estonia (58°17'N, 27°17'E; 38 m.a.s.l.; 1.72 ha). Measurements for Articles I (study period October 2020 – December 2021), II (October 2020 – May 2021), and IV (April – May 2023) were carried out at twelve monitoring points. In Articles I, II, and IV, soil GHG fluxes were determined through continuous gas measurements from automatic soil chambers connected to a Picarro gas analyser. A soil freeze-thaw experiment was conducted in March 2022 for Article III. Heating cables were placed on the ground inside soil collars for flux measurements to induce thawing of the frozen topsoil layer. Gas samples were collected manually from static soil chambers and later analysed by gas chromatography. Stem fluxes were determined by measuring gas concentrations in chambers attached to stems of downy birch (*Betula pubescens*) and Norway spruce (*Picea abies*). Chambers were placed at heights of 0.1, 0.8, and 1.7 m above ground to characterise the vertical profile of stem fluxes. Stem fluxes were quantified from gas samples collected manually once a week and analysed by gas chromatography (Articles I and II). In Article IV, GHG concentrations in the stem chambers were captured on-site using portable Li-Cor gas analysers. Environmental parameters were

measured simultaneously with fluxes. Soil was sampled for chemical and microbial analysis.

Soil at the study site constituted a net annual sink of atmospheric CH<sub>4</sub>, and a source of N<sub>2</sub>O and CO<sub>2</sub>. Higher water table depth (WTD) and soil water content (SWC) kept CH<sub>4</sub> fluxes near-zero during the dormant season, indicating a balance between methanogenesis and methanotrophy in the soil. Substantial CH<sub>4</sub> uptake was observed during the drier summer months, as methanotrophy became more prevalent. However, the relationships between CH<sub>4</sub> fluxes and soil environmental variables were reversed in the springtime study, suggesting that soil hydrology had a significant long-term impact on soil CH<sub>4</sub> dynamics, while temperature can be a more direct governing factor in the short term. Temporal dynamics of soil N<sub>2</sub>O fluxes were driven by hot moments of emissions, induced by rapid changes in SWC, such as freeze-thaw events. The freeze-thaw experiment showed that soil thawing increased N<sub>2</sub>O emissions, initially through nitrification, followed by incomplete denitrification under prolonged anaerobic conditions, evidenced by changes in the microbial community composition. Findings from the spring, reflecting conditions following the freeze-thaw cycle, demonstrated significant changes in the abundances of functional genes between measurement days. Annual soil CO<sub>2</sub> efflux showed near-zero fluxes during the dormant season and increased fluxes during the growing season. Forest floor CO<sub>2</sub> efflux was driven by air and soil temperatures on all measured timescales, relating to the growing season and plant physiological activity.

The first annual measurements of tree stem GHG fluxes in a drained peatland forest were presented. Tree stems were net emitters of all gases, with only spruce stems showing negligible N<sub>2</sub>O uptake. Birch stems played a greater role in the annual GHG dynamics than spruce stems. Inter-species differences could be related to microtopography, gas concentrations in soil water, rooting characteristics, and xylem structures. Temporal dynamics of stem CH<sub>4</sub> and N<sub>2</sub>O fluxes were driven by isolated emissions' peaks. The highest CH<sub>4</sub> flux peak in late June coincided with the end of the wetter period, where sustained higher water levels and increasing soil temperatures created optimal conditions for methanogenesis in the soil. Birch N<sub>2</sub>O emissions' peaks in autumn and spring, triggered by rapid hydrological changes, accounted for 94.9% of the annual flux. The spring peak coincided with the hot moment of soil N<sub>2</sub>O release, induced by freeze-thaw cycles. However, the spring results indicated that under stable SWC conditions optimal for soil N<sub>2</sub>O production, temperature predominantly influenced fluxes. Stem CO<sub>2</sub> release followed a seasonal trend, highly dependent on temperature, as well as solar radiation during spring, suggesting temperature sensitivity of stem respiration and the impact of photosynthesis and the associated tree growth on respiration.

The vertical stem flux profile and fluxes' correlation with soil environmental parameters provide insight into the ongoing challenge of stem fluxes' origin. The net stem CH<sub>4</sub> flux may have been an aggregate of soil-derived and stem-produced CH<sub>4</sub>, with the former originating from deeper soil layers where methanogenesis occurs. A more dominant soil source was evident for birch stem N<sub>2</sub>O fluxes, and

stem CO<sub>2</sub> efflux were likely also related to belowground sources. Comparison of stem and soil flux contributions to their combined fluxes showed that CH<sub>4</sub> emitted from tree stems can offset nearly a third of the soil sink annually, rising to almost half during the wetter period, emphasising the strong longer-term effect of soil hydrological conditions on stem and soil CH<sub>4</sub>. Stem flux contribution to total annual N<sub>2</sub>O emissions remained low regardless of wet or dry periods, highlighting that stem N<sub>2</sub>O fluxes better respond to short-term hydrological changes, rather than seasonal variations. Stem fluxes contributed significantly to the total CO<sub>2</sub> release both during drier and wetter periods, being driven by temperature, rather than seasonal hydrological differences. The findings of these studies underscored that neglecting stem fluxes can lead to inaccurate estimations of forest GHG budgets.

## SUMMARY IN ESTONIAN

### Keskkonnatingimuste ja mulla mikrobioomi mõju kasvuhoonegaaside voogudele hemiboraalse kõdusoometsa mullast ja puutüvedest

Turbaalad katavad umbes kolm protsenti globaalsest maismaa territooriumist, kuid talletavad ligi kolmandiku kogu maailma süsinikust ja kuni veerandi lämmastikust. Nende süsiniku- ja lämmastikuvarude tasakaalu rikkumine võib oluliselt mõjutada peamiste kasvuhoonegaaside (KHG) – süsinikdioksiidi ( $\text{CO}_2$ ), metaani ( $\text{CH}_4$ ) ja dilämmastikoksiidi ehk naerugaasi ( $\text{N}_2\text{O}$ ) – ajalis-ruumilist dünaamikat, mõjutades seeläbi kohalikke biogeokeemilisi ringeid ning andes hoogu globaalsetele kliimamuutustele. Põhjamaades, sealhulgas Eestis, on looduslikke turbaalaseid aastakümneid kuivendatud, peamiselt põllumajandus- või metsamaade rajamiseks. Drenaaž muudab turvasmuldade veerežiimi, mis on oluline KHG-de tasakaalu reguleeriv tegur. Kui looduslikud turbaalad on üldiselt  $\text{CO}_2$  sidujad, mõõdukad  $\text{CH}_4$  allikad ja väikesed  $\text{N}_2\text{O}$  allikad, võib põhjaveetaseme alandamine nad muuta  $\text{CO}_2$  allikateks, vähendada  $\text{CH}_4$  heitkoguseid ja suurendada  $\text{N}_2\text{O}$  eraldumist. Turbaalade pideval kuivendamisel on tõenäoliselt kliimat soojendav mõju, sest vabanev  $\text{CO}_2$  ja  $\text{N}_2\text{O}$  heitkogus ületab  $\text{CH}_4$  emissiooni vähenemisest saadava kiirgusliku toime kahanemise. Lisaks mullale mõjutavad metsanduslikel eesmärkidel kuivendatud turbaalade ehk kõdusoometsade KHG bilansse ka puutüved. Puutüvede rolli KHG allikatena on vähe uuritud ning nende gaasivoogude dünaamika on keeruline. Leidub vähe uuringuid, kus on keskendunud mulla ja puutüvede KHG voogude samaaegsetele pikaajalistele mõõtmistele kõdusoometsades. Varasemad uuringud on mõõtmisi läbi viinud peamiselt kasvu- ja talveperioodil, jättes tähelepanuta sesoonsed varieeruvused, nagu kevadised külmumis- ja sulamistsükliid.

Sellest lähtuvalt on käesoleva doktoritöö eesmärk iseloomustada mulla ja puutüvede KHG voogude aasta- ja aastavahevahelisi variatsioone ja peamisi mõjutavaid keskkonnategureid Eesti kõdusoometsas. Lisaks uuriti töös mullakeemia ja mikroobikoosluste mõju KHG voogudele ning tüvevoogude päritolu. Doktoritöös määrati mulla ja puutüvede  $\text{CH}_4$ ,  $\text{N}_2\text{O}$  ja  $\text{CO}_2$  voogude kogused parasvöötme kõdusoometsas ühe aasta jooksul (Artikkel I), keskendudes eraldi varem alauuritud talveperioodile (Artikkel II). Kuna artiklites I ja II tõusis esile kevadiste külmumis- ja sulamisperioodide tähtsus, viidi läbi mulla soojendamise katse (Artikkel III), uurimaks  $\text{N}_2\text{O}$  emissiooniprotsesse ning mulla mikroobikooslusi külmumis- ja sulamistsükliite ajal. Lisaks uuriti kevadisel kasemahla jooksmise perioodil puutüvede ja mulla KHG voogusid ning nende seost kasemahlas ja mullavees lahustunud gaaside sisalduse ning mulla mikroobikooslustega (Artikkel IV).

Uuring viidi läbi Eesti idaosas Agali kõdusoometsas ( $58^{\circ}17'N$ ,  $27^{\circ}17'E$ ; 38 m; 1,72 ha). Artiklite I (uuringuperiood oktoober 2020 – detsember 2021), II (oktoober 2020–mai 2021) ja IV (aprill–mai 2023) mõõtmised toimusid kaheteistkümnes seirepunktis. Artiklites I, II ja IV määrati mulla KHG vood pidevate automaatmõõtmistega mullakambritest, mis olid ühendatud Picarro gaasianalü-

saatoriga. Artikli III jaoks viidi 2022. aasta märtsis läbi pinnase külmumis-sulamiskatse. Selleks kasutati küttegaasid, mis paigaldati mullavoogude mõõtmiste jaoks pinnasesse installeeritud rõngaste sisse, tagamaks külmunud pinnasekihi perioodilise sulamine. Artiklis III koguti gaasiproovid mullakambritest käsitsi ning analüüsiti hiljem gaasikromatograafiaga. Tüvevoogude määramiseks kinnitati tüvekambriid sookaskede ja (*Betula pubescens*) harilike kuuskede (*Picea abies*) tüvedele 0,1, 0,8 ja 1,7 m kõrgusele maapinnast, et iseloomustada tüvevoo vertikaalset profiili. Tüvevood kvantifitseeriti gaasiproovidest, mis koguti käsitsi kord nädalas puutüvedele paigaldatud kambriüsteemidest ning analüüsiti gaasikromatograafi abil (Artiklid I ja II). Artiklis IV mõõdeti tüvekambrite KHG-de kontsentratsioone kaasaskantavate Li-Cor gaasianalüsaatoritega kohapeal. Samaaegselt voogudega mõõdeti keskkonna- ja meteoroloogilisi parameetreid ning koguti mullaproove füüsikalise-keemiliseks analüüsiks ja mikroobikoosluste määramiseks.

Uuritud kõdusoometsa mulla aastakeskmise bilanss näitas CH<sub>4</sub> sidumist ning N<sub>2</sub>O ja CO<sub>2</sub> lendumist. Talvisel perioodil, kui veetase oli kõrgem, jäid mulla CH<sub>4</sub> vood nullilähedaseks, osutades tasakaalule metanogeneesi ja metanotroofia vahel mullas. Suvel, kui muld oli kuivem, suurenes CH<sub>4</sub> sidumine, kuna metanotroofid muutusid aktiivsemaks ning metanogeneesi mulla ülemises kihis oli pärsitud. Kevadises uuringus muutusid seosed CH<sub>4</sub> voogude ja mulla keskkonnaparameetrite vahel vastupidiseks – temperatuur mängis voogude dünaamikas suuremat rolli kui veeparameetrid. See näitab, et mulla veerežiim omab pikaajalist mõju mulla CH<sub>4</sub> dünaamikale, samas kui temperatuur on olulisem lühiajalises perspektiivis. Mulla N<sub>2</sub>O voogude ajalise dünaamika iseloomustasid emissioonide piigid ehk „kuumad hetked“, mille põhjustasid kiired muutused mullaniiskuses, näiteks külmumis-sulamis tsüklite käigus. Külmutamise-sulatamise katse näitas, et mulla pinnasekihi sulatamine suurendas mullaniiskust ja N<sub>2</sub>O heitkoguseid. Sulamisprotsessi alguses suurenesid vood nitrifikatsiooni kaudu, kuid anaeroobsete tingimuste süvenedes hakkas domineerima mittetäielik denitrifikatsioon, mida kinnitasid muutused mikroobikooslustes. Kevadise uuringu tulemused, mis peegeldasid külmumis-sulamis tsüklile järgnenud tingimusi, näitasid olulisi mõõtmispäevadevahelisi muutusi funktsionaalsete geenide arvukuses. Kiired muutused mikroobikooslustes viitavad vajadusele suurendada proovivõtu sagedust, et täpsemalt määrata KHG voogusid mõjutavad mikrobioloogilised tegurid mullas, eriti lühiajaliste emissioonide piikide ajal. Mulla aastane CO<sub>2</sub> bilanss näitas nullilähedast voogu talveperioodil ja suurenenud heitkoguseid kasvuperioodil. Mulla CO<sub>2</sub> vood olid peamiselt mõjutatud õhu- ja mullatemperatuurist, näidates, et vood sõltuvad oluliselt kasvuperioodist ja taimede füsioloogilisest aktiivsusest.

Artiklis I esitleti esmakordselt aastasi puutüvede KHG voogude mõõtmistulemusi kõdusoometsast. Puutüved olid nii CH<sub>4</sub>, N<sub>2</sub>O kui CO<sub>2</sub> allikad, ainult kuuse tüved näitasid minimaalset N<sub>2</sub>O sidumist. Kase tüvedest pärit KHG emissioonid mängisid aastases KHG dünaamikas suuremat rolli kui kuuse tüvedest pärit vood. Taolised liikidevahelised erinevused võivad tuleneda uurimisala mikrotopograafiast, lahustunud gaaside kontsentratsioonist mullavees, puude

juurestiku sügavusest ja tihedusest ning puu ksüleemi struktuuride erinevustest. Täiendavad uuringud peaksid keskenduma küsimusele, kuidas liigispetsiifilised tunnused mõjutavad gaasi transporti mullast läbi puutüve atmosfääri. Antud töös leiti, et puutüvede CH<sub>4</sub> ja N<sub>2</sub>O voogude ajalised dünaamikad iseloomustasid lühiajalised emissioonide piigid. CH<sub>4</sub> voo piik juuni lõpus langes kokku märja perioodi lõpuga, kus püsivalt kõrge veetase ja kerkiv mullatemperatuur loid optimaalsed tingimused metanogeneesiks. Kase N<sub>2</sub>O emissiooni tipud sügisel ja kevadel, mis on tingitud kiiretest hüdroloogilistest muutustest, moodustasid 94,9% aastases koguvoo. Kevadine N<sub>2</sub>O emissiooni piik langes kokku ka mullas täheldatud „kuuma hetkega“, mille põhjustasid külmumis-sulamistsükli. Kevadise uuringu tulemused aga näitasid, et stabiilse, N<sub>2</sub>O tootmiseks optimaalse, mullaniiskusega muutub temperatuur peamiseks voogusid mõjutavaks teguriks. Sarnaselt mullavoogudele sõltus tüve CO<sub>2</sub> emissioon suuresti temperatuurist, samuti päikesekiirguse intensiivsusest, mis näitab tüve hingamise temperatuuritundlikkust ning fotosünteesi ja sellega kaasneva puude kasvu mõju hingamisele. Tihedam mõtmissagedus aitaks täpsemalt tabada olulisi tüve emissiooni piike, selgitamaks nende põhjuseid ning suurendades teadmisi tüvevoogude panusest metsade KHG-de aastasesse bilanssi.

Tüvevoogude muutused tüve vertikaalsel profiilil ning voogude seosed mulla keskkonnaparameetritega aitavad selgitada tüvevoogude päritolu. Tulemuste alusel võib eeldada, et tüve CH<sub>4</sub> koguvoo võib olla kombinatsioon mullast pärinevast ja tüves toodetud metaanist. Kuna muld oli CH<sub>4</sub> siduja, pärines tüvesse juurte ja ksüleemi kaudu saabuv metaan tõenäoliselt sügavamatest mullakihtidest, kus toimub metanogenees. Tüvedest emiteeruv N<sub>2</sub>O ja CO<sub>2</sub> pärinesid tõenäoliselt peamiselt mullast.

Antud töö näitab, et tüvevoogude väljajätmine metsa KHG-de bilansi hinnangutest võib põhjustada metsa koguheidete üle- või alahindamist. Puutüvedest eralduv CH<sub>4</sub> võib aastas tühistada ligi kolmandiku mulla CH<sub>4</sub> sidumise efektist. Märjemal perioodil võib see osakaal tõusta 50%-ni koguemissioonist, näidates pikaajaliste mullahüdroloogiliste tingimuste tugevat mõju tüvede ja mulla CH<sub>4</sub> voogudele. Tüvevoo panus aastasesse N<sub>2</sub>O heitkogustesse püsis madalal, sõltumata märgadest või kuivadest perioodidest. See viitab, et tüve N<sub>2</sub>O voog reageerib paremini lühiajalistele hüdroloogilistele muutustele, mitte sesoonsetele variatsioonidele. CO<sub>2</sub> puhul mängib tüvevoog olulist rolli, lisades märkimisväärse koguse koguemissiooni nii kuivematel kui niiskematel perioodidel. CO<sub>2</sub> dünaamika on enim sõltuv temperatuurist, mitte sesoonsetest hüdroloogilistest erinevustest.

Antud doktoritöös tõusis esile mulla- ja tüvevoogude lühiajaliste emissiooni- piikide osatähtsus KHG-de aastases bilansis. Seetõttu on tulevikus oluline suurendada mõtmissagedust sesoonsetes uuringutes, et täpsemini tabada emissiooni varieeruvust. Täpsemate vooandmete kombineerimine mullakeemia ja mikroobi-kooslustega aitab paremini määrata vooge seletavat geneetilist potentsiaali.

## ACKNOWLEDGEMENTS

I want to express my sincere gratitude to my supervisors Assoc. Prof. Kaido Soosaar and Prof. Ülo Mander. First, for giving me the opportunity to join the team back in 2020, for their continuous support and guidance throughout the past years, and for providing me with countless opportunities for professional development. I am, of course, most grateful for the opportunities to join fieldwork expeditions to Malaysia, Peru, and many other exciting places. Absolute highlights of my PhD journey that kept the motivation high!

This PhD would not have been possible without the excellent team behind the projects. I want to thank all co-authors for their help and contributions. Special thanks go to Dr Thomas Schindler for being my primary mentor in fieldworks, Dr Jordi Escuer-Gatius for his continuous help with data analysis, and Anto Raig, Mart Muhel and Dr Alar Teemusk for making the field station and laboratory analysis run smoothly. I would also like to acknowledge my fellow PhD students in the department – it has been wonderful to share the highs and lows of this journey with such an inspiring group.

A special thank you also goes to my family. To my parents, for igniting a curiosity for the world and for supporting my crazy dreams. To my younger sisters, for reminding me to be a good role model. I would not have followed a scientific career if it wasn't for my extended family. I got my love for geography from my dad's side of the family and my interest in science from my mum's side. An excellent combination that has led me to embark on the most exciting professional endeavours. And finally, a huge thank you to the best group of friends, each of them being a source of inspiration in their own different way.

The studies in this doctoral thesis were supported by the Ministry of Education and Science of Estonia (SF0180127s08 grant), the Estonian Research Council (IUT2-16, PRG352, PRG1434, PRG2032, MOBERC20, MOBERC44), Infrastructures R&D project “Estonian Environmental Observatory”, SustES – Adaptation strategies for sustainable ecosystem services and food security under adverse environmental conditions (CZ.02.1.01/0.0/0.0/16\_019/ 0000797), AnaEE Estonia Project (2014–2020.4.01.20-0285) funded by the EU Regional Development Fund, and the EU through the European Regional Development Fund (the Center of Excellence EcolChange and AgroCropFuture). This work was also supported by the European Union Horizon programme under grant agreement No 101079192 (MLTOM23003R) and the European Research Council (ERC) under grant agreement No 101096403 (MLTOM23415R).

## **PUBLICATIONS**

# CURRICULUM VITAE

Name Reti Ranniku  
Date of birth 27.01.1995  
Citizenship Estonian  
E-mail reti.ranniku@ut.ee

## Education

2020–... PhD Physical Geography, University of Tartu, Estonia  
2017–2019 MSc Climate Change, University of Copenhagen, Denmark  
2014–2017 BSc Geography, University of East Anglia, UK

## Employment

01.03.2022–  
30.08.2024 University of Tartu, Faculty of Science and Technology,  
Institute of Ecology and Earth Sciences, Junior Research Fellow  
in Physical Geography  
2019–2020 University of Copenhagen, Centre for Permafrost, Research and  
Laboratory Assistant

## Fields of research

Biogeochemistry, climate change, physical geography, soil science, greenhouse gases

## Awarded scholarships

Kristjan Jaak scholarship for participation at the AGU Fall Meeting 2021 in New Orleans, US  
Jaan-Mati Punning scholarship for young researchers in physical geography, 2022  
Dora Pluss scholarship for participation at the EGU General Assembly 2022 in Vienna, Austria  
Kristjan Jaak scholarship for participation at the BIOGEMON conference in 2024 in San Juan, Puerto Rico, US

## Publications

**Ranniku, R.**, Mander, Ü., Escuer-Gatius, J., Schindler, T., Kupper, P., Sellin, A., Soosaar, K. (2024) Dry and wet periods determine stem and soil greenhouse gas fluxes in a northern drained peatland forest. *Science of the Total Environment*. 928, 172452. <https://doi.org/10.1016/j.scitotenv.2024.172452>  
Kazmi, F.A., Espenberg, M., Pärn, J., Masta, M., **Ranniku, R.**, Thayamkottu, S., Mander, Ü. (2023) Meltwater of freeze-thaw cycles drives N<sub>2</sub>O-governing microbial communities in a drained peatland forest soil. *Biology and Fertility of Soils*. <https://doi.org/10.1007/s00374-023-01790-w>

- Ranniku, R.**, Schindler, T., Escuer-Gatius, J., Mander, Ü., Machacova, K., Soosaar, K. (2023) Tree stems are a net source of CH<sub>4</sub> and N<sub>2</sub>O in a hemiboreal drained peatland forest during the winter period. *Environmental Research Communications*, 5, 051010.  
<https://doi.org/10.1088/2515-7620/acd7c7>
- Mander, Ü., Krasnova, A., Schindler, T., Megonigal, J. P., Escuer-Gatius, J., Espenberg, M., Machacova, K., Maddison, M., Pärn, J., **Ranniku, R.**, Pihlatie, M., Kasak, K., Niinemets, Ü., Soosaar, K. (2022) Long-term dynamics of soil, tree stem and ecosystem methane fluxes in a riparian forest. *Science of the Total Environment*, 809, 151723.  
<https://doi.org/10.1016/j.scitotenv.2021.151723>
- Wang, P., D'Imperio, L., Biersma, E. M., **Ranniku, R.**, Xu, W., Tian, Q., Ambus, P., Elberling, B. (2020) Combined effects of glacial retreat and penguin activity on soil greenhouse gas fluxes on South Georgia, sub-Antarctica. *Science of The Total Environment*, 718, 135255.  
<https://doi.org/10.1016/j.scitotenv.2019.135255>

## ELULOOKIRJELDUS

Nimi Reti Ranniku  
Sünniaeg 27.01.1995  
Kodakondsus Eesti  
E-post reti.ranniku@ut.ee

### Haridus

2020–... PhD Loodusgeograafia, Tartu Ülikool, Eesti  
2017–2019 MSc Kliimamuutused, Kopenhaageni Ülikool, Taani  
2014–2017 BSc Geograafia, East Anglia Ülikool, Suurbritannia

### Teenistuskäik

01.03.2022–  
30.08.2024 Tartu Ülikool, Loodus- ja täppisteaduste valdkond, ökoloogia ja maateaduste instituut, loodusgeograafia nooremteadur  
2019–2020 Kopenhaageni Ülikool, Centre for Permafrost, Laboriassistent

### Teadussuunad

Biogeokeemia, kliimamuutused, loodusgeograafia, mullateadus, kasvuhoonegaasid

### Stipendiumid

Kristjan Jaagu õpirände stipendium osalemaks konverentsil AGU Fall Meeting 2021 asukohas New Orleans, US  
Jaan-Mati Punningu nimeline stipendium noorteadlastele loodusgeograafia erialal, 2022  
Dora Pluss õpirände stipendium osalemaks konverentsil EGU General Assembly 2022 asukohas Viin, Austria  
Kristjan Jaagu õpirände stipendium osalemaks konverentsil BIOGEOMON 2024 asukohas San Juan, Puerto Rico, US

### Publikatsioonid

**Ranniku, R.**, Mander, Ü., Escuer-Gatius, J., Schindler, T., Kupper, P., Sellin, A., Soosaar, K. (2024) Dry and wet periods determine stem and soil greenhouse gas fluxes in a northern drained peatland forest. *Science of the Total Environment*. 928, 172452. <https://doi.org/10.1016/j.scitotenv.2024.172452>  
Kazmi, F.A., Espenberg, M., Pärn, J., Masta, M., **Ranniku, R.**, Thayamkottu, S., Mander, Ü. (2023) Meltwater of freeze-thaw cycles drives N<sub>2</sub>O-governing microbial communities in a drained peatland forest soil. *Biology and Fertility of Soils*. <https://doi.org/10.1007/s00374-023-01790-w>

- Ranniku, R.**, Schindler, T., Escuer-Gatius, J., Mander, Ü., Machacova, K., Soosaar, K. (2023) Tree stems are a net source of CH<sub>4</sub> and N<sub>2</sub>O in a hemiboreal drained peatland forest during the winter period. *Environmental Research Communications*, 5, 051010. <https://doi.org/10.1088/2515-7620/acd7c7>
- Mander, Ü., Krasnova, A., Schindler, T., Megonigal, J. P., Escuer-Gatius, J., Espenberg, M., Machacova, K., Maddison, M., Pärn, J., **Ranniku, R.**, Pihlatie, M., Kasak, K., Niinemets, Ü., Soosaar, K. (2022) Long-term dynamics of soil, tree stem and ecosystem methane fluxes in a riparian forest. *Science of the Total Environment*, 809, 151723. <https://doi.org/10.1016/j.scitotenv.2021.151723>
- Wang, P., D'Imperio, L., Biersma, E. M., **Ranniku, R.**, Xu, W., Tian, Q., Ambus, P., Elberling, B. (2020) Combined effects of glacial retreat and penguin activity on soil greenhouse gas fluxes on South Georgia, sub-Antarctica. *Science of The Total Environment*, 718, 135255. <https://doi.org/10.1016/j.scitotenv.2019.135255>.

## DISSERTATIONES GEOGRAPHICAE UNIVERSITATIS TARTUENSIS

1. **Вийви Руссак.** Солнечная радиация в Тыравере. Тарту, 1991.
2. **Urmas Peterson.** Studies on Reflectance Factor Dynamics of Forest Communities in Estonia. Tartu, 1993.
3. **Ülo Suursaar.** Soome lahe avaosa ja Eesti rannikumere vee kvaliteedi analüüs. Tartu, 1993.
4. **Kiira Aaviksoo.** Application of Markov Models in Investigation of Vegetation and Land Use Dynamics in Estonian Mire Landscapes. Tartu, 1993.
5. **Kjell Wepling.** On the assessment of feasible liming strategies for acid sulphate waters in Finland. Tartu, 1997.
6. **Hannes Palang.** Landscape changes in Estonia: the past and the future. Tartu, 1998.
7. **Eiki Berg.** Estonia's northeastern periphery in politics: socio-economic and ethnic dimensions. Tartu, 1999.
8. **Valdo Kuusemets.** Nitrogen and phosphorus transformation in riparian buffer zones of agricultural landscapes in Estonia. Tartu, 1999.
9. **Kalev Sepp.** The methodology and applications of agricultural landscape monitoring in Estonia. Tartu, 1999.
10. **Rein Ahas.** Spatial and temporal variability of phenological phases in Estonia. Tartu, 1999.
11. **Эрки Таммиксаар.** Географические аспекты творчества Карла Бэра в 1830–1840 гг. Тарту, 2000.
12. **Garri Raagmaa.** Regional identity and public leaders in regional economic development. Tartu, 2000.
13. **Tiit Tammaru.** Linnastumine ja linnade kasv Eestis nõukogude aastatel. Tartu, 2001.
14. **Tõnu Muring.** Wastewater treatment wetlands in Estonia: efficiency and landscape analysis. Tartu, 2001.
15. **Ain Kull.** Impact of weather and climatic fluctuations on nutrient flows in rural catchments. Tartu, 2001.
16. **Robert Szava-Kovats.** Assessment of stream sediment contamination by median sum of weighted residuals regression. Tartu, 2001.
17. **Heno Sarv.** Indigenous Europeans east of Moscow. Population and Migration Patterns of the Largest Finno-Ugrian Peoples in Russia from the 18<sup>th</sup> to the 20<sup>th</sup> Centuries. Tartu, 2002.
18. **Mart Külvik.** Ecological networks in Estonia — concepts and applications. Tartu, 2002.
19. **Arvo Järvet.** Influence of hydrological factors and human impact on the ecological state of shallow Lake Võrtsjärv in Estonia. Tartu, 2004.
20. **Katrin Pajuste.** Deposition and transformation of air pollutants in coniferous forests. Tartu, 2004.

21. **Helen Sooväli.** *Saaremaa waltz*. Landscape imagery of Saaremaa Island in the 20th century. Tartu, 2004.
22. **Antti Roose.** Optimisation of environmental monitoring network by integrated modelling strategy with geographic information system — an Estonian case. Tartu, 2005.
23. **Anto Aasa.** Changes in phenological time series in Estonia and Central and Eastern Europe 1951–1998. Relationships with air temperature and atmospheric circulation. Tartu, 2005.
24. **Anneli Palo.** Relationships between landscape factors and vegetation site types: case study from Saare county, Estonia. Tartu, 2005.
25. **Mait Sepp.** Influence of atmospheric circulation on environmental variables in Estonia. Tartu, 2005.
26. **Helen Alumäe.** Landscape preferences of local people: considerations for landscape planning in rural areas of Estonia. Tartu, 2006.
27. **Aarne Luud.** Evaluation of moose habitats and forest reclamation in Estonian oil shale mining areas. Tartu, 2006.
28. **Taavi Pae.** Formation of cultural traits in Estonia resulting from historical administrative division. Tartu, 2006.
29. **Anneli Kährik.** Socio-spatial residential segregation in post-socialist cities: the case of Tallinn, Estonia. Tartu, 2006.
30. **Dago Antov.** Road user perception towards road safety in Estonia. Tartu, 2006.
31. **Üllas Ehrlich.** Ecological economics as a tool for resource based nature conservation management in Estonia. Tartu, 2007.
32. **Evelyn Uuema.** Indicatory value of landscape metrics for river water quality and landscape pattern. Tartu, 2007.
33. **Raivo Aunap.** The applicability of gis data in detecting and representing changes in landscape: three case studies in Estonia. Tartu, 2007.
34. **Kai Treier.** Trends of air pollutants in precipitation at Estonian monitoring stations. Tartu, 2008.
35. **Kadri Leetmaa.** Residential suburbanisation in the Tallinn metropolitan area. Tartu, 2008.
36. **Mare Remm.** Geographic aspects of enterobiasis in Estonia. Tartu, 2009.
37. **Alar Teemusk.** Temperature and water regime, and runoff water quality of planted roofs. Tartu, 2009.
38. **Kai Kimmel.** Ecosystem services of Estonian wetlands. Tartu, 2009.
39. **Merje Lesta.** Evaluation of regulation functions of rural landscapes for the optimal siting of treatment wetlands and mitigation of greenhouse gas emissions. Tartu, 2009.
40. **Siiri Silm.** The seasonality of social phenomena in Estonia: the location of the population, alcohol consumption and births. Tartu, 2009.
41. **Ene Indermitte.** Exposure to fluorides in drinking water and dental fluorosis risk among the population of Estonia. Tartu, 2010.
42. **Kaido Soosaar.** Greenhouse gas fluxes in rural landscapes of Estonia. Tartu, 2010.

43. **Jaan Pärn.** Landscape factors in material transport from rural catchments in Estonia. Tartu, 2010.
44. **Triin Saue.** Simulated potato crop yield as an indicator of climate variability in Estonia. Tartu, 2011.
45. **Katrin Rosenvald.** Factors affecting EcM roots and rhizosphere in silver birch stands. Tartu, 2011.
46. **Ülle Marksoo.** Long-term unemployment and its regional disparities in Estonia. Tartu, 2011, 163 p.
47. **Hando Hain.** The role of voluntary certification in promoting sustainable natural resource use in transitional economies. Tartu, 2012, 180 p.
48. **Jüri-Ott Salm.** Emission of greenhouse gases CO<sub>2</sub>, CH<sub>4</sub>, and N<sub>2</sub>O from Estonian transitional fens and ombrotrophic bogs: the impact of different land-use practices. Tartu, 2012, 125 p.
49. **Valentina Sagris.** Land Parcel Identification System conceptual model: development of geoinfo community conceptual model. Tartu, 2013, 161 p.
50. **Kristina Sohar.** Oak dendrochronology and climatic signal in Finland and the Baltic States. Tartu, 2013, 129 p.
51. **Riho Marja.** The relationships between farmland birds, land use and landscape structure in Northern Europe. Tartu, 2013, 134 p.
52. **Olle Järv.** Mobile phone based data in human travel behaviour studies: New insights from a longitudinal perspective. Tartu, 2013, 168 p.
53. **Sven-Erik Enno.** Thunderstorm and lightning climatology in the Baltic countries and in northern Europe. Tartu, 2014, 142 p.
54. **Kaupo Mändla.** Southern cyclones in northern Europe and their influence on climate variability. Tartu, 2014, 142 p.
55. **Riina Vaht.** The impact of oil shale mine water on hydrological pathways and regime in northeast Estonia. Tartu, 2014, 111 p.
56. **Jaanus Veemaa.** Reconsidering geography and power: policy ensembles, spatial knowledge, and the quest for consistent imagination. Tartu, 2014, 163 p.
57. **Kristi Anniste.** East-West migration in Europe: The case of Estonia after regaining independence. Tartu, 2014, 151 p.
58. **Piret Pungas-Kohv.** Between maintaining and sustaining heritage in landscape: The examples of Estonian mires and village swings. Tartu, 2015, 210 p.
59. **Mart Reimann.** Formation and assessment of landscape recreational values. Tartu, 2015, 127 p.
60. **Järvi Järveoja.** Fluxes of the greenhouse gases CO<sub>2</sub>, CH<sub>4</sub> and N<sub>2</sub>O from abandoned peat extraction areas: Impact of bioenergy crop cultivation and peatland restoration. Tartu, 2015, 171 p.
61. **Raili Torga.** The effects of elevated humidity, extreme weather conditions and clear-cut on greenhouse gas emissions in fast growing deciduous forests. Tartu, 2016, 128 p.
62. **Mari Nuga.** Soviet-era summerhouses On homes and planning in post-socialist suburbia. Tartu, 2016, 179 p.

63. **Age Poom.** Spatial aspects of the environmental load of consumption and mobility. Tartu, 2017, 141 p.
64. **Merle Muru.** GIS-based palaeogeographical reconstructions of the Baltic Sea shores in Estonia and adjoining areas during the Stone Age. Tartu, 2017, 132 p.
65. **Ülle Napa.** Heavy metals in Estonian coniferous forests. Tartu, 2017, 129 p.
66. **Liisi Jakobson.** Mutual effects of wind speed, air temperature and sea ice concentration in the Arctic and their teleconnections with climate variability in the eastern Baltic Sea region. Tartu, 2018, 118 p.
67. **Tanel Tamm.** Use of local statistics in remote sensing of grasslands and forests. Tartu, 2018, 106 p.
68. **Enel Pungas.** Differences in Migration Intentions by Ethnicity and Education: The Case of Estonia. Tartu, 2018, 142 p.
69. **Kadi Mägi.** Ethnic residential segregation and integration of the Russian-speaking population in Estonia. Tartu, 2018, 173 p.
70. **Kiira Mõisja.** Thematic accuracy and completeness of topographic maps. Tartu, 2018, 112 p.
71. **Kristiina Kukk.** Understanding the vicious circle of segregation: The role of leisure time activities. Tartu, 2019, 143 p.
72. **Kaie Kriiska.** Variation in annual carbon fluxes affecting the soil organic carbon pool and the dynamics of decomposition in hemiboreal coniferous forests. Tartu, 2019, 146 p.
73. **Pille Metspalu.** The changing role of the planner. Implications of creative pragmatism in Estonian spatial planning. Tartu, 2019, 128 p.
74. **Janika Raun.** Mobile positioning data for tourism destination studies and statistics. Tartu, 2020, 153 p.
75. **Birgit Viru.** Snow cover dynamics and its impact on greenhouse gas fluxes in drained peatlands in Estonia. Tartu, 2020, 123 p.
76. **Iuliia Burdun.** Improving groundwater table monitoring for Northern Hemisphere peatlands using optical and thermal satellite data. Tartu, 2020, 162 p.
77. **Ingmar Pastak.** Gentrification and displacement of long-term residents in post-industrial neighbourhoods of Tallinn. Tartu, 2021, 141 p.
78. **Veronika Mooses.** Towards a more comprehensive understanding of ethnic segregation: activity space and the vicious circle of segregation. Tartu, 2021, 161 p.
79. **Johanna Pirrus.** Contemporary Urban Policies and Planning Measures in Socialist-Era Large Housing Estates. Tartu, 2021, 142 p.
80. **Gert Veber.** Greenhouse gas fluxes in natural and drained peatlands: spatial and temporal dynamics. Tartu, 2021, 210 p.
81. **Anniki Puura.** Relationships between personal social networks and spatial mobility with mobile phone data. Tartu, 2021, 144 p.
82. **Alisa Krasnova.** Greenhouse gas fluxes in hemiboreal forest ecosystems. Tartu, 2022, 185 p.

83. **Tauri Tampuu.** Synthetic Aperture Radar Interferometry as a tool for monitoring the dynamics of peatland surface. Tartu, 2022, 166 p.
84. **Najmeh Mozaffaree Pour.** Urban Expansion in Estonia: Monitoring, Analysis, and Modeling. Tartu, 2022, 169 p.
85. **Bruno Montibeller.** Evaluating human-induced forest degradation in different biomes using spatial analysis of satellite-derived data. Tartu, 2022, 112 p.
86. **Holger Virro.** Geospatial data harmonization and machine learning for large-scale water quality modelling. Tartu, 2022, 138 p.
87. **Azadeh Rezapour.** The impact of climate change on fine root trait responses of deciduous and coniferous trees. Tartu, 2023, 108 p.
88. **Isaac Newton Kwasi Buo.** Multi-scale thermal Remote Sensing, Machine Learning, and Radiative Flux Modeling to Assess Urban Overheating. Tartu, 2023, 116 p.
89. **David Knapp.** The relationship between residential segregation, school segregation and family context. Tartu, 2024, 122 p.